City-scale information modelling for urban energy resilience with optimal battery energy storages in Hong Kong

Ping, Dazhou; Li, Chaosu; Yu, Xiaojun; Liu, Zhengxuan; Tu, Ran; Zhou, Yuekuan

DOI
10.1016/j.apenergy.2024.124813

Publication date
2025

Document Version
Final published version

Published in
Applied Energy

Applied Energy 378 (2025) 124813

Contents lists available at ScienceDirect

Applied Energy

journal homepage: www.elsevier.com/locate/apenergy

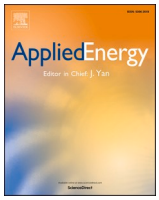

City-scale information modelling for urban energy resilience with optimal battery energy storages in Hong Kong

Dazhou Ping [a,b], Chaosu Li [a,c,*], Xiaojun Yu [b], Zhengxuan Liu [d], Ran Tu [e], Yuekuan Zhou [b,f,g,h,**]

[a] Urban Governance and Design Thrust, The Hong Kong University of Science and Technology (Guangzhou), Guangzhou 511400, China
[b] Sustainable Energy and Environment Thrust, The Hong Kong University of Science and Technology (Guangzhou), Guangzhou 511400, China
[c] Division of Public Policy, The Hong Kong University of Science and Technology, China
[d] Faculty of Architecture and the Built Environment, Delft University of Technology, Julianalaan 134, 2628 BL, Delft, Netherlands
[e] School of Transportation, Southeast University, Nanjing 210096, China
[f] Department of Mechanical and Aerospace Engineering, The Hong Kong University of Science and Technology, Clear Water Bay, Hong Kong, SAR, China
[g] HKUST Shenzhen-Hong Kong Collaborative Innovation Research Institute, Futian, Shenzhen, China
[h] Division of Emerging Interdisciplinary Areas, The Hong Kong University of Science and Technology, Clear Water Bay, Hong Kong, SAR, China

HIGHLIGHTS

- A city-scale information model with renewable and storage for energy resilience.
- A GIS-MCDM approach for optimal BESS deployment with locations and capacities.
- Urban-scale resilience with geological, safety, energy flexibility and accessibility.
- Spatiotemporal resolution urban energy simulation for power shortage reduction.
- Guidelines for designers and planners with energy resilience and power survivability.

ARTICLE INFO

Keywords:
Urban energy resilience
Geographic information system
Multi-criteria decision-making
Battery energy storage systems
District power shortage
Urban-scale deployment planning

ABSTRACT

Climate change and extreme weather events are imposing threats to city power systems with regional power shortages. To enhance urban power system's resilience amid climate change, photovoltaic (PV) and battery energy storage systems (BESS) are crucial for maintaining self-sufficient power during outages. However, the optimal installation location and capacity sizing of BESS remain uncertain when considering multi-criteria, including safety, energy flexibility, accessibility and energy resilience. This study proposes a new approach, i.e., Geographic Information System (GIS) integrated with Multi-Criteria Decision-Making (MCDM) and capacitated p-median problem, to identify optimal installation locations and capacity allocation of BESS. This approach comprehensively considers geographical conditions (such as slope, land use, open space), safety, energy flexibility, accessibility and energy resilience, while accounting for the entire distribution network's granularity, intermittent solar supply, and unstable electricity demand. The methodology can guide the optimal BESS siting and sizing for energy resilience under future climate change and associated extreme weather events. Results indicate that suitable installation locations based on the proposed GIS-MCDM method are concentrated in central and southern regions in Yau Tsim Mong. Subsequently, BESS with the optimal and specific installation location and capacity allocation is in districts with high electricity demand and favourable safety geographical conditions. Compared to BESS without GIS-MCDM, the optimal BESS deployment with GIS-MCDM decreases the power shortage from 13,184 MWh to 12,931 MWh. Additionally, it increases the maximum power shortage reduction density from 176.04 kWh/m^2 to 364.2 kWh/m^2, and the area with a power shortage reduction above 100 kWh/m^2 expands from 1.24 $\times$ 10^5 m^2 to 2.17 $\times$ 10^5 m^2. This study contributes a new approach to determine optimal

* Corresponding author at: Urban Governance and Design Thrust, Society Hub, The Hong Kong University of Science and Technology (Guangzhou), Guangzhou 511400, Guangdong, China.
** Corresponding author at: Sustainable Energy and Environment Thrust, Function Hub, The Hong Kong University of Science and Technology (Guangzhou), Guangzhou 511400, Guangdong, China.
E-mail addresses: chaosuli@hkust-gz.edu.cn (C. Li), yuekuan.zhou@outlook.com (Y. Zhou).

https://doi.org/10.1016/j.apenergy.2024.124813
Received 14 July 2024; Received in revised form 19 September 2024; Accepted 27 October 2024
Available online 5 November 2024

BESS installation locations and capacity allocation in urban-scale information modelling, planning and deployment, with frontier guidelines for system designers and urban planners to collaboratively develop resilience and survivability of urban power systems under extreme events.

Nomenclature

Variables (units)

C	Cost for BESS investment (HK$)
C_{CAPEX}	Capital expenditure cost of BESS (HK$/kWh)
$C_{shortage}$	Power shortage cost (HK$/kWh)
Cap	Capacity of BESS (MWh)
d	Euclidean distance (m)
e	Entropy value
h	Bandwidth (m)
$Loss_{shortage}$	Economic losses for power shortage (HK$)
NP_{BESS}	Net profit of BESS (HK$)
K	Gaussian kernel function
$P_{charging}(t)$	Charging power at time step t (MW)
$P_{discharging}(t)$	Discharging power at time step t (MW)
$P_{shortage}(t)$	Power shortage at time step t (MW)
$Pr_{grid}(t)$	Time-of-use grid price in Hong Kong (HK$/kWh)
R	Power shortage ratio
$Revenue_{BESS}$	Revenue of BESS (HK$)
t	Time duration of extreme events (h)
v	Wind speed (m/s)
w	Weight of each criterion

Abbreviations

BESS	Battery energy storage system
CPMP	Capacitated P-Median Problem
ED	Electricity demand
EUI	Energy use intensity
GIS	Geographical information system
KDE	Kernel density estimation
MCDM	Multi-criteria decision-making
POI	Point of interest
PV	Photovoltaic
SCR	Self-consumption ratio
SSR	Self-sufficiency ratio

Sets

n	Set of candidate BESS installation locations
p	Set of selected BESS installation locations

1. Introduction

Climate change has become a major issue for sustainable development goals [1], leading to increased energy consumption and energy shortage crisis [2,3]. Energy resilience is critical for sustaining power systems under future climate change risks and the associated extreme events [4,5]. To address these challenges, high penetration of renewable energy sources and energy-efficient utilization are essential strategies to mitigate climate change and enhance climate-adaptive resilience [6]. However, it still remains a significant challenge to determine where to locate and how to design clean energy supply and battery storage systems with high energy resilience to withstand the impacts of extreme weather events.

Addressing the challenges posed by climate change requires comprehensive approaches in many aspects, particularly in terms of management strategies with renewable energy. One of the major issues with solar power generation is its sensitivity to climate and weather-induced intermittency, which makes it particularly vulnerable to extreme weather events and compromises the resilience of power systems [7]. For onsite renewable integrated building prosumers, climate change will not only affect the dynamic electricity consumption, but also affect the onsite renewable energy supply. For example, from the energy consumption aspect, Moazami et al. [8] quantified the building performance under long-term climate change and extreme weather conditions. They indicated that typical database would underestimate peak load, and the extreme weather will improve the robust design in buildings. Berardi and Jafarpur [9] studied the change of cooling and heating loads under climate change. The case study indicates that rise in temperature will reduce the Heating Degree Days by 30 %, reduce the energy use intensity (EUI) for heating by 18–33 %, and increase EUI for cooling by 15 %–126 %. Flores-Larsen et al. [10] investigated the impact of climate change on energy consumption from 2020 to 2050, and concluded that heating energy is decreased by 6.0–7.6 kWh/m^2·decade, while the cooling energy is increased by 1.7–8.4 kWh/m^2·decade. From the clean energy supply aspect, Feron et al. [11] assessed the variation of PV production with global climate models (RCP4.5 and RCP8.5). They found that, during summer days, PV power outputs are expected to double in the Arabian Peninsula by mid-century, while PV power outputs can be reduced by half in southern Europe over the same period, even under a moderate-emission scenario. Zhao et al. [12] evaluated the impacts of climate change on PV energy potential based on the downscaled climate projections in China. Results indicate that PV-energy potential is likely to have a slight decrease of up to 6 % in most of the study regions under RCP4.5 and RCP8.5. However, under the urban scale, the impact of climate change on variations of electricity demands and PV production has not been considered, especially considering different building types and forms, leading to suboptimal urban planning decisions without considering energy resilience and, therefore, the ineffectiveness of traditional integrated urban energy strategies.

To address this risk, flexible and effective deployment of battery energy storage system (BESS) is imperative to enable rapid charging/discharging and offer substantial storage capacity to smooth fluctuations in electricity supply across various locations and strategies [13,14]. Some studies have already highlighted the importance of BESS deployment in power systems. For instance, the deployment of energy storage systems can help reduce carbon emissions by facilitating renewable energy integration and improving the overall efficiency of the power system [15,16]. Moreover, battery efficiency is significant in improving energy resilience under power outages and extreme winds, respectively [17,18]. The primary objective of the BESS in this situation is to enhance grid resilience by storing excess PV and grid electricity. This stored energy reduces the risk of power shortages during disasters, ensuring continuity of power supply to critical loads and essential services during extreme events. Through the efficient utilization of renewable energy, the BESS contributes to the stability and resilience of the energy system, particularly in high-risk scenarios. However, traditional methods for battery deployment under the theoretical modelling approach fail to consider geographical conditions (like slope, land use, public open space, and so on), safety, energy flexibility, accessibility and energy resilience, leading to the ineffectiveness in practical applications.

Geographic Information System (GIS)-assisted site selection on clean

energy supply and energy storages under the urban scale can improve the practical applications [19] and efficiency of decision-making processes [20], with comprehensive considerations on various factors, such as geography, topography, land use, etc. Precise site selection on clean energy supply and energy storage through spatial analysis and modelling based on GIS can consider the geological conditions, accessibility, and regional energy demand, enabling its effectiveness and practicability [20]. Additionally, GIS can be used to assess potential risks and initiate emergency response plans, so as to improve energy resilience of the entire power system [21]. Researchers have already applied GIS for site allocation on clean energy systems. Alhamwi et al. [22] introduced a GIS-based platform to optimize the allocation of distributed battery storage in urban areas. Wei et al. [23] proposed a city-scale PV deployment decision-making model and evaluated the deployment potential that 100 % deployment targets can achieve 20.6 % of the city's electricity demand considering the real installation conditions under the urban scale. Ren et al. [24] proposed a 3D-GIS and deep learning integrated approach to solve the high-dimensional rooftop PV planning problem and the non-linear PV and battery sizing problem with the minimum payback period. Zhou et al. [25] proposed a practical model for the location decision of PV charging stations, combining GIS with multi-criteria decision-initiate emergency response plan-making methods. As intermediate battery storage between clean energy supply and end-users' demand, the effective BESS deployment has to consider not only geographical conditions, but also complex interactions among PV, end-users, and the local power grid. Challenges of battery deployment arise from the complexity of multi-directional power interactions among multi-agents, especially for large city-scale information. A climate-adaptive PV-BESS power system with high energy resilience is highly necessary to guide battery deployment in terms of optimal installation locations and capacity allocation on an urban scale.

Based on the above literature review, scientific gaps are summarised below:

(1) Traditional BESS deployment methods only focus on optimizing storage capacity and cost efficiency from technical and economic aspects, lacking practical geographical consideration for urban-scale networks. Up until now, there is no methodology for BESS deployment under the urban scale, considering the complex spatiotemporal relationship among PV production, electricity demand and BESS.
(2) In response to mitigating future climate change and surviving the power system under extreme weather, the roles of BESS deployment to enhance the energy resilience of the power system have not been specifically explored, especially considering the complexity and sophistication from the perspective of the spatiotemporal distribution of building electricity demand and PV production under the urban scale.
(3) Traditional performance assessment for the BESS deployment is normally limited within the integrated technical criteria, such as self-consumption ratio and self-sufficiency, which cannot adequately reflect the spatial performance of BESS deployment. However, performance assessment for BESS from the spatial perspective under an urban scale has not been proposed yet.

In order to fill up the identified scientific gaps, the research originality and novelty of this study are shown below:

(1) A novel GIS-MCDM approach is developed to identify the suitable BESS installation ranges. Besides considering the geographical criterion for safety and accessibility, a criterion specifically for energy resilience (i.e., distance to increased electricity demand) has been first proposed to emphasize the significant connection between the BESS deployment and requirement for the electricity demand in the power system.
(2) Optimal BESS deployment with specific installation locations and capacity allocation are identified to enhance energy resilience under climate change and extreme events. It integrates high-resolution spatiotemporal data (i.e., PV production, building electricity demand, optimal BESS deployment) to develop a power system with high energy resilience under urban scale. Moreover, extreme weather events have been simulated to assess the effectiveness and robustness of the proposed BESS deployment strategy.
(3) Power shortage reduction density based on the kernel density estimation has been innovatively applied to evaluate the energy resilience of the power system from the spatial perspective. Furthermore, with the power shortage mitigation as the temporal assessment criteria, energy resilience of the power system with the proposed optimal BESS deployment has been thoroughly evaluated from spatial and temporal aspects.

This study is organised as follows. Research methodology is described in Section 2. Results and discussion are given in Section 3. Furthermore, Section 3 also shows the limitations and future outlook. Lastly, the conclusion of this study is presented in Section 4.

2. Methodology

Fig. 1 illustrates the framework for optimal site selection and capacity sizing and allocation on battery energy system storage (BESS), together with a multi-criteria performance assessment. In the first stage, various data are collected and processed, including environmental data, building data, and urban infrastructure data, which will be integrated into a GIS-based platform for spatial analysis. In the second stage, the energy system simulation is conducted, encompassing building energy simulation, solar radiance, and PV production simulation. This stage involves parameter setting (such as building geometry, window-to-wall ratio, thermophysical properties of materials, etc), meteorological parameters, and solar-to-power conversions. A comprehensive suitability map is thereafter generated with suitability criteria, energy resilience and energy flexibility through GIS-based multi-criteria decision-making (MCDM). In the third stage, a capacitated p-median problem solution is employed to optimize the location and allocate the capacity of the PV-battery systems.

The study aims to minimize the demand-weighted distance between demand nodes and PV-BESS facilities, considering energy resilience to survive the power system against extreme weather events. The demand-weighted distance method was chosen due to its simplicity and effectiveness in prioritizing areas with high electricity demand. This approach ensures that Battery Energy Storage Systems (BESS) are located where they will have the greatest impact on grid resilience and efficiency, especially in urban areas. Unlike other weighting methods that may only consider proximity or provide equal weight across regions, demand-weighted distance emphasizes demand magnitude, leading to more effective BESS placement. Compared to multi-objective optimization methods, demand-weighted distance offers a less computationally intensive solution while still ensuring that the BESS is placed in regions of high demand. Although multi-objective methods can incorporate additional factors, demand-weighted distance directly targets the most critical parameter, energy demand, which leads to efficient and impactful storage system placement.

2.1. Geographical information on the study area

(Note: This figure presents a two-part geographic illustration of Yau Tsim Mong District in Hong Kong. The left panel provides a regional map highlighting the district's location within the larger context of Hong Kong. The right panel offers a detailed urban map of Yau Tsim Mong, showcasing a dense network of buildings and roads.)

As shown in Fig. 2, Yau Tsim Mong District in Hong Kong is selected

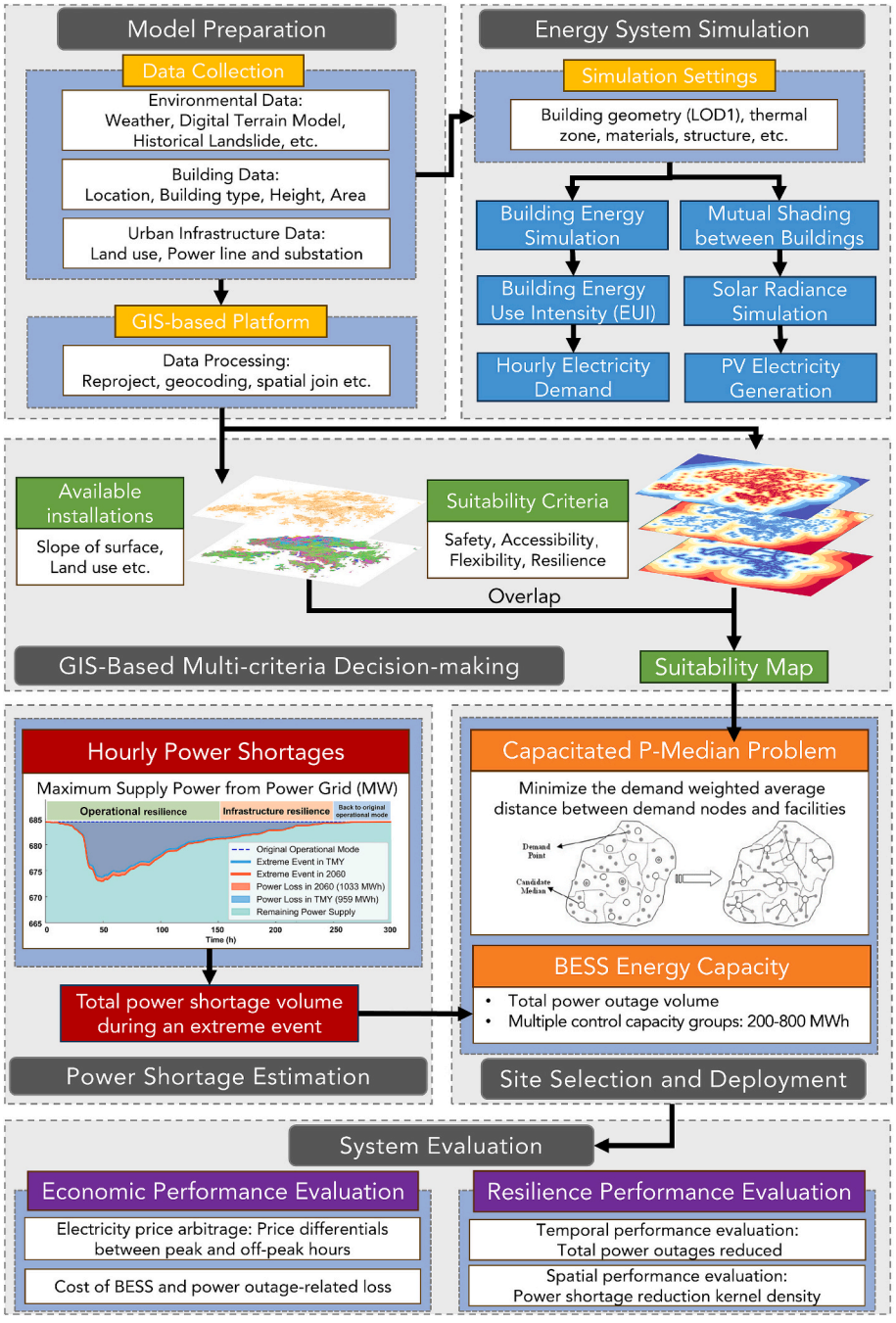

Fig. 1. Flow chart of research methodology on optimal site selection and multi-criteria performance assessment on battery energy system storage (BESS).

in this study as a research area. The district is situated at the heart of Kowloon Peninsula as one of the most bustling regions and is known for its high density of population and commercial activities. The district features a diverse array of buildings, including high-rise office buildings, residential buildings, and commercial buildings, which provides great potential for PV installation on the rooftop and building façade, thereby maximumly enhancing the energy resilience of the power system.

2.2. Urban energy simulation and PV production estimation

In this research, offices, hotels, and residences are selected as three typical buildings to present all types of buildings, and their dynamic energy use intensity (EUI) is simulated in TRNSYS [26–30], which temporally provides dynamic electricity demands. Energy use intensity (EUI) for these three types of buildings is calculated as the baseline, and actual electricity demand is expanded through the calculated EUI and scaled according to different building areas and building types. Building height and building area are obtained from Amap [31], which provides accurate shape file data from a spatial aspect. Additionally, the identification of building types was achieved by integrating land cover data from the Planning Department and Point of Interest (POI) data from Amap [31]. This comprehensive approach ensures that the energy electricity models are precise and representative, corresponding to the actual building conditions from spatiotemporal aspects under the urban scale.

For the estimation of PV production, the Climate Studio Grasshopper plugin is utilized to model the hourly solar radiation on building surfaces, taking into account the mutual shading effect among the

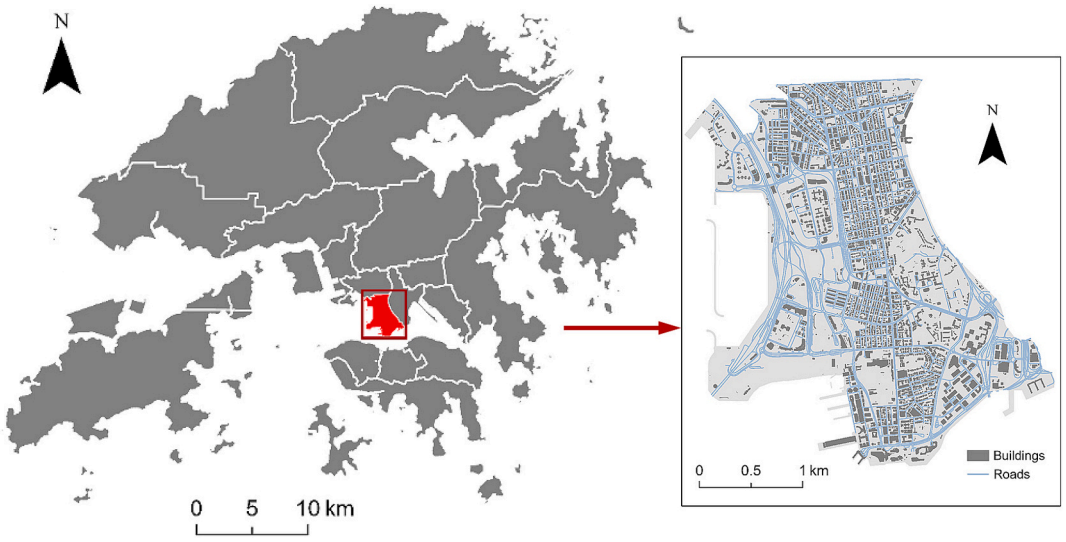

Fig. 2. Geographical location of Yau Tsim Mong in Hong Kong.

buildings. Each building is modelled at Level of Detail 1 [32], which is assumed that 80 % of the building facades and rooftop are covered by PV installations, with PV energy efficiency rate under the standard testing condition at 20 % [33]. Furthermore, the impact of shading among buildings and climate change on the hourly PV production is specifically quantified.

2.3. Simulation of power shortage under extreme weather event

To estimate the impact of extreme weather events on power shortages in Hong Kong, a predictive model is developed utilizing detailed power outage data from catastrophic windstorms in Miami, United States [34]. Miami is chosen for several key reasons. First, both Miami and Hong Kong are frequently affected by intense tropical cyclones—hurricanes and typhoons, respectively—with similar characteristics such as high wind speeds, heavy rainfall, and storm surges [35,36]. This similarity in storm impact makes Miami's outage data relevant for modelling purposes in Hong Kong. Second, both cities share comparable urban characteristics, including high population density, extensive high-rise developments, and complex infrastructure systems [37,38]. These factors influence the vulnerability and resilience of power systems in similar ways, affecting how extreme weather events impact power supply [39]. Third, Miami provides detailed and publicly available power outage data from past windstorms, which is not readily available for Hong Kong or other comparable cities. This data availability allows for a more robust modelling approach. It is acknowledged that there are differences in power system configurations between Miami and Hong Kong. To address this, the data in Miami-Dade is analysed and then integrated with Hong Kong's meteorological and power grid characteristics through linear regression to create a tailored predictive model for Hong Kong's power shortage simulation based on its specific conditions. Specifically, the impact of power outages in Hong Kong during Typhoon Mangkhut was considered, and the power shortage ratio are modified accordingly [40,41].

Previous studies have found that power shortage caused by the catastrophic windstorm is highly related to the wind speed and time duration of the disaster [39]. This model incorporates two variables (i.e., wind speed and time duration) to quantify the power shortage during catastrophic windstorms. Power shortage ratio (R) is defined as the percentage of the population in the power shortage area affected by the catastrophic windstorm relative to the total population. It is modelled as a two-variable function related to wind speed (v) and time duration (t), as shown in Eq. (1):

$$R_{\text{Miami-Dade,U.S}} = 0.0040 \times v + 0.0078 \times t - 0.081 \quad (1)$$

where R refers to power shortage ratio [40]. v refers to the wind speed (m/s), and t refers to the time duration (h) of the extreme event.

Based on the principles of external validity, power shortage data from Miami during catastrophic windstorms can be extrapolated to predict power shortage conditions in Hong Kong under extreme events. Therefore, power shortage ratio in Hong Kong ($R_{\text{Hong Kong}}$) can be obtained by multiplying power shortage ratio in Miami by a coefficient (as shown in Eq. (2)).

$$R_{\text{Hong Kong}} = a \times (0.0040 \times v + 0.0078 \times t - 0.081) \quad (2)$$

This coefficient *a* is calculated as the ratio of the proportion of population affected by power outages in Hong Kong to that in Miami, which is expressed as:

$$a = \frac{\left(\text{Population under power shortage}_{\text{Hong Kong}} \Big/ \text{Total population}_{\text{Hong Kong}}\right)}{\left(\text{Population under power shortage}_{\text{Miami}} / \text{Total population}_{\text{Miami}}\right)} \quad (2.1)$$

where population under power shortage equals to 10,800 in Hong Kong [41] and 898,340 in Miami [34], while total population equals to 7,346,000 in Hong Kong [42] and 2,701,767 in Miami [43]. In Eq. (2.1), the metric "population under power shortage" refers primarily to power shortages caused by catastrophic wind storms. These storms are considered the dominant factor affecting grid resilience in this study, given their high likelihood and severe impact in the regions. Other causes of shortages are not explicitly included, as during such large-scale outages, other causes like equipment malfunctions or random failures are statistically insignificant.

Fig. 3 shows the power shortage ratio in Miami-Dade overtime during a storm event. Miami-Dade experiences a sharp increase in outage ratios, peaking early in the event, followed by a gradual recovery over approximately 260 h. This trend can be used as the benchmark for the resilience evaluation of Hong Kong's power infrastructure during extreme events.

2.4. Urban BESS deployment through GIS-MCDM

After identifying the spatiotemporal electricity demand and PV production under urban scale, BESS requires to be deployed to maximumly increase the energy resilience of the power system. Fig. 4 shows the schematic diagram of the optimal BESS deployment, which follows a

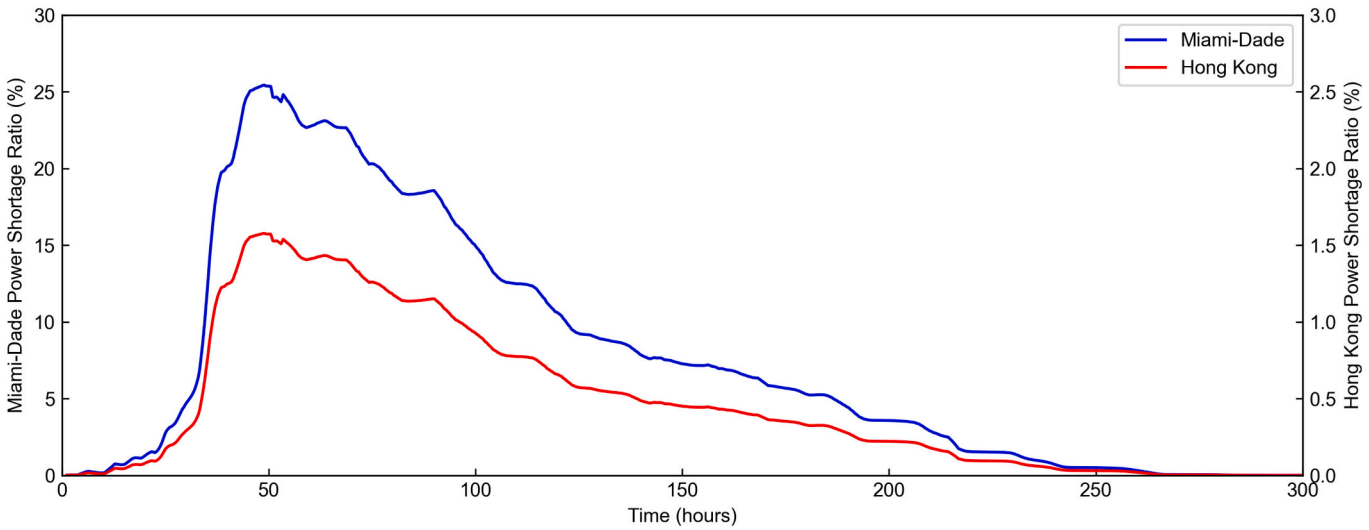

Fig. 3. Power shortage ratio in Miami and Hong Kong under catastrophic windstorm.

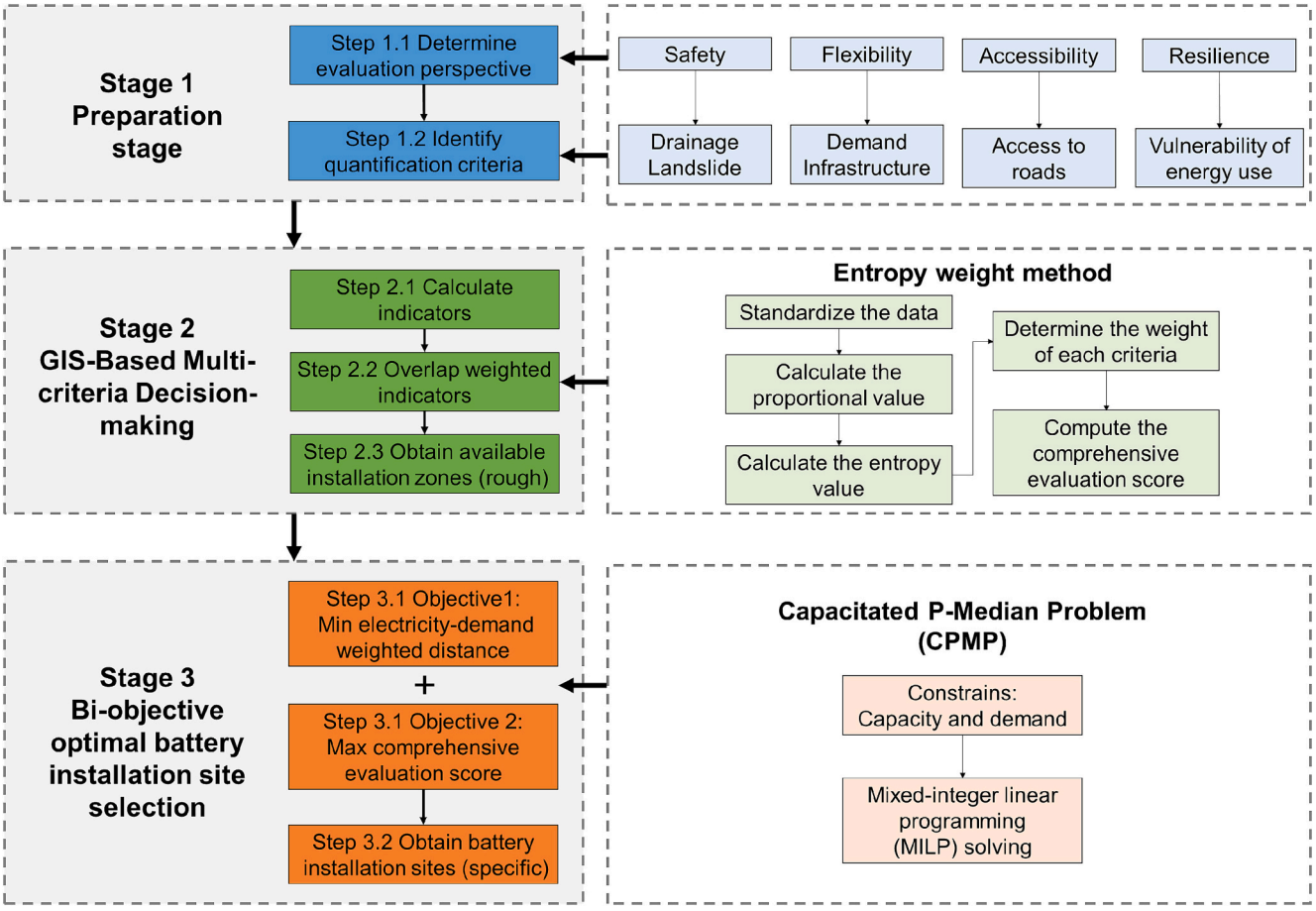

Fig. 4. Flow chart of the optimal BESS deployment process.

three-stage sequence (i.e., Stage I: data preparation stage for evaluation perspectives and criteria, Stage II: GIS-based multi-criteria decision-making for the identification of rough feasible installation range, and Stage III: bi-objective optimal site selection for the optimal and specific installation location and capacity allocation). By following this method, optimal deployment of BESS can effectively enhance the system's energy resilience, ensuring a robust and adaptable power infrastructure that can withstand and recover from various disruptions. Later subsections will elaborate on each step in details, respectively.

2.4.1. Multi-criteria decision-making (MCDM) and entropy weight method for feasible BESS installation locations

Before identifying the specific optimal location, feasible installation locations need to be roughly determined to ensure alignment with actual urban geographic conditions and to reduce the computational load of the subsequent BESS optimization. This helps to streamline the process

by narrowing down potential sites, thereby making the final selection more efficient and practical.

In order to firstly identify the rough feasible BESS installation locations, criteria for feasible installation locations need to be identified, to exclude those infeasible installation locations from the map. Table 1 outlines the standard utilized in this research to exclude infeasible locations based on slope, land use, public open space, and proximity to critical water sources. These standards ensure that only physically suitable and safe locations are considered for BESS installations. Locations that do not follow the standard should be excluded to avoid the installation accident.

After excluding infeasible areas based on the standards shown in Table 1, remaining feasible areas should be further evaluated to identify more suitable sites. To achieve this target, a robust multi-criteria decision-making (MCDM) framework is further developed to evaluate the suitability potential of remaining locations based on criteria such as safety, accessibility, flexibility, and resilience (as shown in Table 2). Fig. 5 shows the source geographical data for assessing the feasibility and suitability of urban BESS installation related to criteria, as listed in Table 2. Criteria for safety, flexibility and accessibility are regulated from standards [44,45]. Furthermore, criterion for energy resilience is measured as the distance to the increased electricity demand, which indicates that distance closer to the increased electricity demand should be considered with a high priority, while distance far away from the increased electricity demand is considered with a low priority.

In order to identify areas that are more susceptible to climate change, spatial differences in building electricity demands under typical and 2060 are quantified. These differences are primarily driven by meteorological parameters' change, variations in air temperature and building density. Fig. 6 demonstrates the detailed calculation process for the energy resilience criterion. First, land surface temperature in Yau Tsim Mong is collected from Landsat-8 Land Surface Temperature (LST) product [46]. Based on a temperature conversion model [47], land surface temperature can be converted to the air temperature. Then, air temperature datasets from several key weather stations in Kowloon, including King's Park, Kowloon City, Sham Shui Po, and the Hong Kong Observatory, are selected to obtain high-resolution (10-min interval) temperature records from July 18 to August 1 in 2022. These air temperature datasets are used to calibrate and validate the temperature conversion model. Afterward, Yau Tsim Mong (study area in this research) is divided into 100 m × 100 m grids, and each grid's building density is determined using detailed urban planning datasets, including building areas and counts. The converted air temperature for Yau Tsim Mong is mapped to each grid, and combined with building models. Electricity demand for the typical year and 2060 are simulated using TRNSYS [26], which accounts for the building density and dynamic air temperature within each grid. Lastly, by comparing the differences in electricity demand across grids between the typical year and 2060, distance to the increased electricity demand can be clearly identified as one of the important criteria for energy resilience assessment.

Based on the criteria above, the spatial suitability distribution of each criterion can be calculated. All criteria need to be comprehensively considered and evaluated, while the priority and rating level of each criterion determine the final decision making to generate more reliable BESS locations. In this research, the Entropy Weight Method is introduced, which is an objective weighting method used in multi-criteria decision making (MCDM) analysis to score the potential locations. This method determines the weight of each criterion by calculating the entropy value, which reflects the uncertainty or variability of the information for each criterion. A higher entropy value indicates that the criterion carries more uncertainty and variability, which gives it more importance in the final decision-making process. Conversely, a lower entropy value suggests that the criterion is more stable and, therefore, less significant in influencing the final decision. Once the weights are determined using the entropy values, the next step is to multiply the score of each individual criterion by its corresponding weight. Based on this process, each criterion's contribution to the overall evaluation is adjusted according to its importance. The higher the weight of a criterion, the more influence it has on the final suitability score. For example, if proximity to demand points has a higher weight, locations closer to high electricity demand areas will score significantly higher compared to those further away. This ensures that critical criteria, such as energy resilience or safety, play a central role in the decision-making process, while less critical criteria exert less influence. Finally, the weighted scores of all the criteria are summed up to obtain a comprehensive score for each potential location, allowing us to prioritize the most suitable sites for BESS deployment. This comprehensive score provides a more accurate and holistic assessment of the suitability of each location based on multiple criteria. Detailed steps and calculation expressions are listed

Table 1
Standards to exclude infeasible installation locations [44].

Standard	Constraint	Description
Slope	Construction accessibility	The site location should be physically suitable for installation and should have a minimum drainage slope of 0.5 %.
Land use	Construction accessibility	The site should not occupy land that is not available for development, such as farmland or green areas.
Public open space	Prevent damage or adverse effect	The site should not occupy public open spaces.
Distance to the river and reservoir	Safety	The site location should not be close to important water sources or water protection areas.

Table 2
Criteria for determining suitable installation locations [44,45].

Category	Criteria	Quantitation	Descriptions
Safety	Drainage	Distance to storm water inlet	The station site should meet the requirements for flood and waterlogging prevention, and it's better to be close to drainage facilities [45].
	Landslide	Distance to location of landslide incidents	The station site should be far away from areas directly threatened by debris flows and landslides [44].
Flexibility	Proximity to demand	Distance to buildings	The station site should be close to the points of electricity demand and renewable energy production. The farther the distance from the connection, the slower the response.
	Proximity to Infrastructure	Distance to power grid	The station site should be close to the substation or land with power lines. The farther the distance from the connection, the slower the response and the higher the cost of the project [45].
Accessibility	Ease of access to roads	Distance to road network	The site should have convenient and cost-effective transportation conditions for installation and maintenance, with short and direct connections to the external roads [44,45].
Resilience	Vulnerability of energy use	Distance to increased electricity demand	The site should near buildings that are more prone to shortages in extreme weather, such as extreme heat.

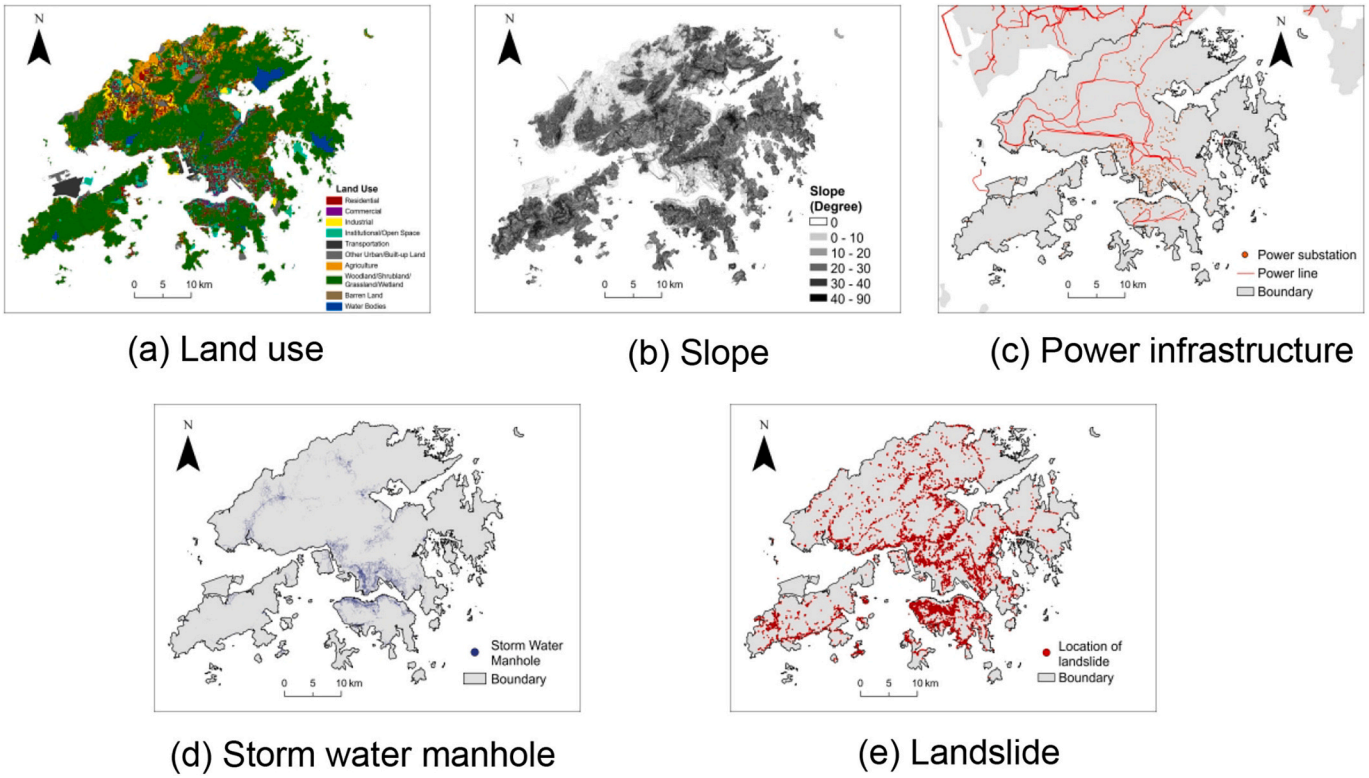

Fig. 5. Geographical data for multi-criteria decision-making (MCDM) analysis based on: (a) land use; (b) slope; (c) power infrastructure; (d) storm water manhole; (e) landslide.

below:

1. Normalized distance performance for each criterion

Transform the distance to a dimensionless scale to facilitate comparison. The formula is expressed as:

$$z_{ij} = \frac{x_{ij} - min(x_{ij})}{max(x_{ij}) - min(x_{ij})} \tag{3}$$

where x_{ij} refers to the distance of sample i and criteria j (as shown in Table 2).

2. Calculate the proportional value

Compute the proportional value p_{ij} of the i^{th} sample in the j^{th} criterion. The formula is:

$$p_{ij} = \frac{z_{ij}}{\sum_{i=1}^{n} z_{ij}} \tag{4}$$

where p_{ij} is the normalized distance of sample i and criteria j ranging from 0 to 1.

3. Calculate the entropy value

Determine the entropy value e_j for each criterion. The formula is:

$$e_j = -\frac{1}{ln(n)} \sum_{i=1}^{n} \left[p_{ij} \bullet ln\left(p_{ij}\right) \right] \tag{5}$$

where n refers to the total amount of sample, and p_{ij} refers to the normalized distance (as shown in Eq. (4)).

4. Determine the weight of each criterion

Calculate the weight w_j for each criterion. The formula is:

$$w_j = \frac{1 - e_j}{\sum_{j=1}^{m} (1 - e_j)} \tag{6}$$

where e_j refers to the entropy weight of criterion j (as shown in Eq. (5)).

5. Compute the comprehensive evaluation score

Calculate the comprehensive evaluation score S_i for each sample. The formula is:

$$S_i = \sum_{j=1}^{m} w_j \cdot p_{ij} \tag{7}$$

where w_j refers to the weight of criterion j (as shown in Eq. (6)), and p_{ij} refers to the normalized distance (as shown in Eq. (4)).

Using these five steps above, entropy weight method can be applied to the geographical data (as shown in Fig. 5) for multi-criteria decision-making (MCDM) analysis with the criteria listed in Table 2 to create a comprehensive suitability map with weighted criteria for evaluating the optimal site.

2.4.2. Optimal BESS deployment with capacitated P-median problem (CPMP)

Battery capacity sizing focuses on ensuring the maximum energy resilience by meeting electricity demand during power shortage periods. In our analysis, the estimated battery energy storage system (BESS) capacity is designed to cover the total power loss over the entire duration of a disaster event, as shown in Fig. 12. This capacity represents the cumulative hourly power loss during a windstorm and assumes that the total storage capacity of the BESS should be at least equal to the

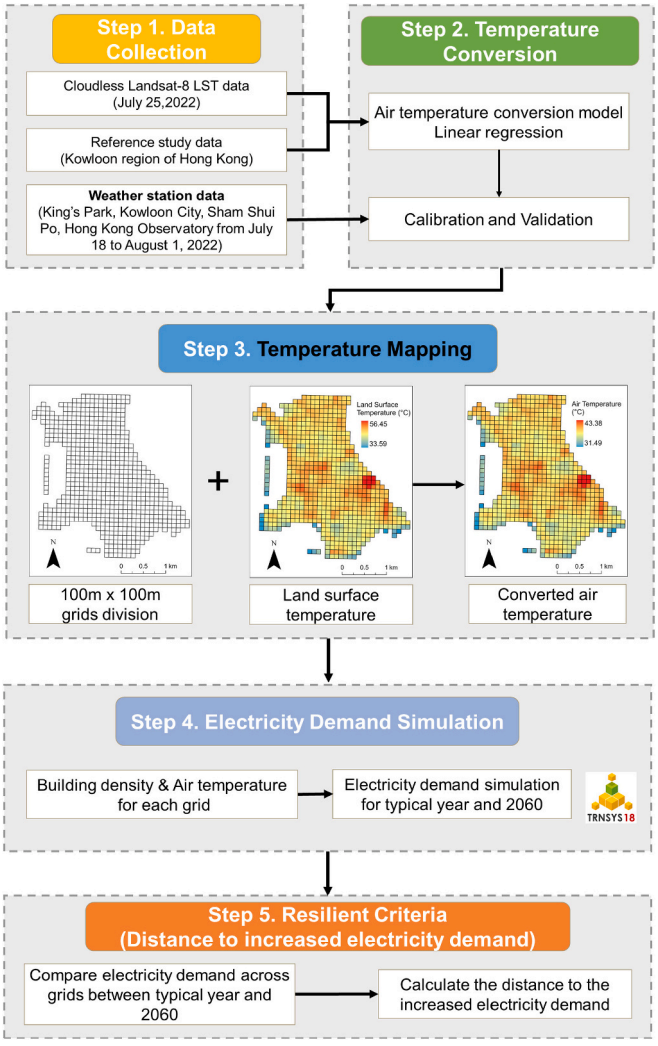

Fig. 6. Flow chart of the calculation process for the energy resilience criterion (i.e., the distance to the increased electricity demand).

difference between electricity demand and PV production:

$$TC_{BESS} = \int_{t_{start}}^{t_{end}} (P_{ED}(t) - P_{PV}(t))dt \tag{8}$$

where t_{start} represents the start time of the extreme event. t_{end} represents the end time of the extreme event. $P_{ED}(t)$ refers to the electricity demand at time step t, and $P_{PV}(t)$ refers to the PV production at time step t. This ensures that the BESS can fully address the most critical power shortages, thereby maximizing energy resilience during grid disruptions. Based on above, sufficient energy services can be fully guarantee during significant grid disruptions.

Capacitated P-median problem [51] aims to solve the optimal BESS deployment, considering distances and capacities for the service between each battery and each building. The objective of the optimized BESS deployment is to determine p (BESS installation locations) in a predefined set with n ($n > p$) candidate BESS installation locations in order to satisfy a set of electricity demands, so that the total sum of road network distances between each electricity demand point (i.e., each building) and its nearest BESS is minimized, which is expressed as:

$$Min \sum_{i=1}^{n} \sum_{j=1}^{n} a_i \cdot d_{ij} \cdot x_{ij} \tag{9}$$

s.t.

$$\sum_{j=1}^{n} x_{ij} = 1, i = 1, 2, \ldots, n \tag{9.1}$$

$$x_{ij} \le y_j, i, j = 1, 2, \ldots, n \tag{9.2}$$

$$\sum_{j=1}^{n} y_j \le p \tag{9.3}$$

$$x_{ij}, y_j \in \{01\}, i, j = 1, 2, \ldots, n \tag{9.4}$$

$$x_{ij} = \begin{cases} 1, \text{when electricity demand of ith building is assigned to jth candidate BESS} \\ 0, \text{otherwise} \end{cases} \tag{9.5}$$

$$y_j = \begin{cases} 1, \text{when jth candidate BESS is selected as one of the optimal BESS locations} \\ 0, \text{otherwise} \end{cases} \tag{9.6}$$

potential power loss. Although the actual state of charge (SOC) of the batteries at the onset of a disaster may not always be at 100 %, the stored energy will still mitigate a significant portion of power outages, providing critical backup power. This approach ensures that the grid can handle the cumulative impact of power shortages over the entire disaster period, rather than focusing solely on short-term. It is determined based on anticipated future risks rather than economic efficiency. Therefore, total capacity of BESS (TC_{BESS}) is designed as the maximum magnitude of the hourly power shortage, which is defined as the maximum

$$Cap_{BESS,j} \le TC_{BESS} \tag{9.7}$$

where n refers to the number of proposed BESS installation locations, and p refers to the candidate BESS installation location selected from proposed BESS installation locations n. a_i refers to the electricity demand of i^{th} building. d_{ij} refers to the road network distance from i^{th} building to j^{th} BESS installation location. x_{ij} is defined as a Boolean variable, where it equals to 1 when electricity demand of i^{th} building is

assigned to j^{th} installed BESS. TC_{BESS} refers to the total BESS capacity that requires to be allocated. $Cap_{BESS,j}$ refers to the allocated BESS capacity for each BESS installation location.

Compared to traditional distance metrics or equal weighting methods, demand-weighted distance offers significant advantages. Simple distance-based methods may place BESS near low-demand areas simply due to their proximity, which would lead to inefficient use of energy storage. Likewise, equal weighting across regions risks ignoring critical high-demand areas, misaligning BESS deployment with actual energy needs. By focusing on demand magnitude alongside proximity, we ensure that BESS placement is directly linked to the areas where the energy grid faces the highest loads. This is especially important in urban settings where electricity demand is often concentrated in specific locations, such as large residential buildings, hospitals, or commercial districts. Consequently, BESS capacity allocation follows the proportion of power shortage, which is defined as:

$$Cap_{BESS,j} = \frac{P_{short,i}}{\sum_{i=1}^{m}(P_{short,i})} \tag{10}$$

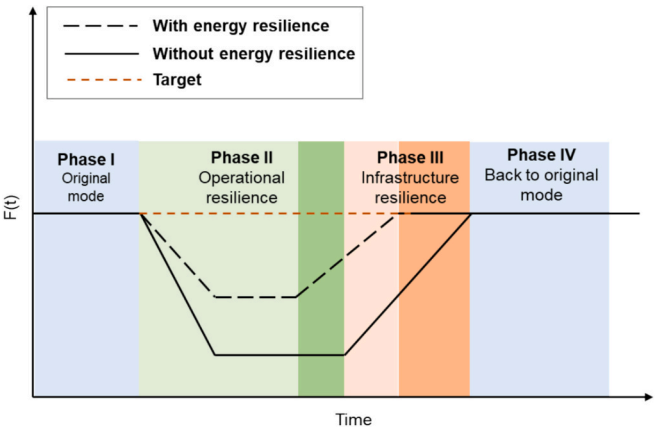

Fig. 7. Performance comparison under conditions with and without energy resilience under stochastic disruptions.

$$P_{short,i} = \begin{cases} ED_i - PV_i, \text{when electricity demand of ith building is greater than ith PV production} \\ 0, \text{otherwise} \end{cases} \tag{10.1}$$

where $P_{short,i}$ refers to the electricity demand shortage when PV production cannot meet the electricity demand of the i^{th} building.

When BESS interacts with the grid, following power network constraints need to be met, including power line constraints, energy balance and storage constraints [52].

(1) Power line constraints: Power line constraints are governed by Kirchhoff's Voltage Law (KVL) in AC networks. Power flows are constrained by power line capacities to prevent overloads, which is expressed as:

$$\left|P_{flow,l}\right| \le P_{max,l} \tag{11}$$

where $P_{flow,l}$ refers to the power flow through line l, and $P_{max,l}$ is the maximum allowed power capacity of that line.

(2) Energy balance: The power injected into the grid is equal the total demand at each bus. This balance is essential to ensure that supply meets demand:

$$\int_{t=0}^{T}\left(P_{PV,i}(t) + P_{BESS\ i,charging}(t) + P_{grid\ imp,i}(t)\right)dt = \int_{t=0}^{T}\left(P_{ED,i}(t) + P_{BESS\ i,discharging}(t) + P_{loss,i}(t) + P_{dumped,i}(t)\right)dt \tag{12}$$

$$\sum_{i=1}^{\text{Total number of buildings}} P_{imp,i} \le P_{grid\ reduced} \tag{13}$$

$$P_{grid\ reduced}(t) = P_{grid\ normal} \times R \tag{14}$$

where $P_{PV,i}(t)$ and $P_{ED,i}(t)$ refer to the the on-site PV generation, electricity demand of building i at time step t, $P_{BESS\ i,charging}(t)$ and $P_{BESS\ i,discharging}(t)$ refer to the charging and discharging power of BESS to building i at time step t. $P_{imp,i}(t)$ refers to the import electricity from the local power grid for shortage electricity demand, and $P_{dumped,i}(t)$ refers to the dumped solar energy generated by PV due to the limited BESS capacity. During the extreme event, the maximum grid import power is reduced from the original transmission capacity ($P_{grid\ normal}$) to a reduced grid import power ($P_{grid\ reduced}$), which is calculated by applying the power shortage ratio (R). Power shortage ratio is calculated in Eq. (1).

(3) Storage Constraints: BESS also follow storage-specific constraints to ensure that their charge and discharge cycles respect capacity limits. The state of charge (SOC) evolves over time as:

$$SOC_i(t) \times Cap_{BESS,i} = SOC_{i-1}(t) \times Cap_{BESS,i} + \eta_{char} \times P_{BESS\ i,charging}(t) - \eta_{dischar} \times P_{BESS\ i,discharging}(t) \tag{15}$$

where $SOC_i(t)$ refers to the state of charge of battery of building i at time step t. $P_{BESS\ i,charging}(t)$ and $P_{BESS\ i,discharging}(t)$ refer to charging and discharging power at time step t. η_{char} and η_{disch}refer to the charging and discharging efficiency, which equal to 95 % [53].

In this research, the proposed BESS installation locations will be selected from pre-determined feasible locations through multi-criteria decision-making and entropy weight method, which greatly increase the resilient of the proposed BESS deployment. By systematically integrating GIS data, energy simulations, decision-making frameworks, capacitated p-median problem for optimal BESS deployment, this study provides a

comprehensive approach to optimize the installation location and capacity allocation for BESS deployment under urban scale, therefore enhancing the resilience of the power system against future extreme weather events.

2.5. Assessment criteria for BESS deployment

In Section 2.4.1, the Entropy Weight Method (EWM) is employed to determine the weights of various criteria influencing the deployment of battery energy storage systems (BESS). This method assigns weights to factors such as proximity to demand points, road accessibility, and power system vulnerability, reflecting their relative importance in the multi-criteria decision-making (MCDM) process. The use of EWM ensures that criteria with greater significance for enhancing energy resilience are given higher priority in the decision-making process. Then in Section 2.4.2, these weights are integrated into the multi-criteria decision-making (MCDM) framework to evaluate the suitability of potential BESS deployment locations. The resulting suitability scores highlight the locations most likely to enhance energy resilience. Subsequently, Section 2.5.1 employs the total power outage reduction and Kernel Density Estimation (KDE) to temporally and spatially evaluate the reduction in power shortages achieved by the deployment of BESS. Then, in section 2.5.2, the economic performance BESS deployments are accessed by their total revenue, costs, and net profits.

2.5.1. The impact of BESS deployment on energy resilience

In order to assess whether the proposed approach on installation location and capacity allocation for BESS deployment is good or not, assessment criteria are proposed from both temporal and spatial perspectives for performance evaluations. From the temporal aspect, energy resilience with the optimal BESS deployment is evaluated with the total amount of power shortage during off-grid operation periods. Fig. 7 demonstrates the schematic diagram of the performance comparison between resilient and traditional power systems under stochastic disruptions. In this research, performance indicator for resilience evaluation is quantified as the accumulated hourly power shortage reduction between conditions with and without energy resilience. Total power outage is expressed as:

$$\text{Total power shortage reduction} = \int_0^{T_d} \left[F(t)_{\text{without energy resilience}} - F(t)_{\text{with energy resilience}} \right] dt \tag{16}$$

where $F(t)_{\text{without energy resilience}}$ represents the power shortage without energy resilience, while $F(t)_{\text{with energy resilience}}$ represents the power shortage with energy resilience.

From the spatial aspect, energy resilience with the optimal BESS deployment is evaluated with kernel density estimation (KDE) for power shortage analysis. KDE is a nonparametric statistical method for estimating the probability density function of a random variable. For the power shortage analysis in this research, KDE is used to identify and evaluate the spatial distribution of power shortages to help identify hotspots and demonstrate the severity of the power shortage problem in each location by calculating the spatial density of power shortage values.

Power shortage reduction kernel density is expressed as:

$$f(xy) = \frac{1}{Nh^2} \sum_{i=1}^{N} K\left(\frac{d_i}{h}\right) \cdot w_i \tag{17}$$

where N refers to the total number of buildings; w_i refers to the value of total power shortages reduced by BESS for building i, and h refers to the bandwidth (m), which is defined as the self-defined search area. K refers to the Gaussian kernel function, which is defined as:

$$K = \frac{1}{\sqrt{2\pi}} exp\left(-\frac{1}{2} \bullet \left(\frac{d_i}{h}\right)^2 \right) \tag{17.1}$$

where d_i refers to the Euclidean distance (m) between the estimated point (x,y) and the i^{th} sample point (x_i,y_i) (sample is defined as building), which is expressed as:

$$d_i = \sqrt{(x - x_i)^2 + (y - y_i)^2} \tag{17.2}$$

With KDE, severity of the power shortage problem can be quantified from the spatial aspect to develop a more targeted power infrastructure for further energy resilience improvements.

2.5.2. Impact of the BESS deployment on the economic performance

Besides the impact of the BESS deployment on the energy resilience

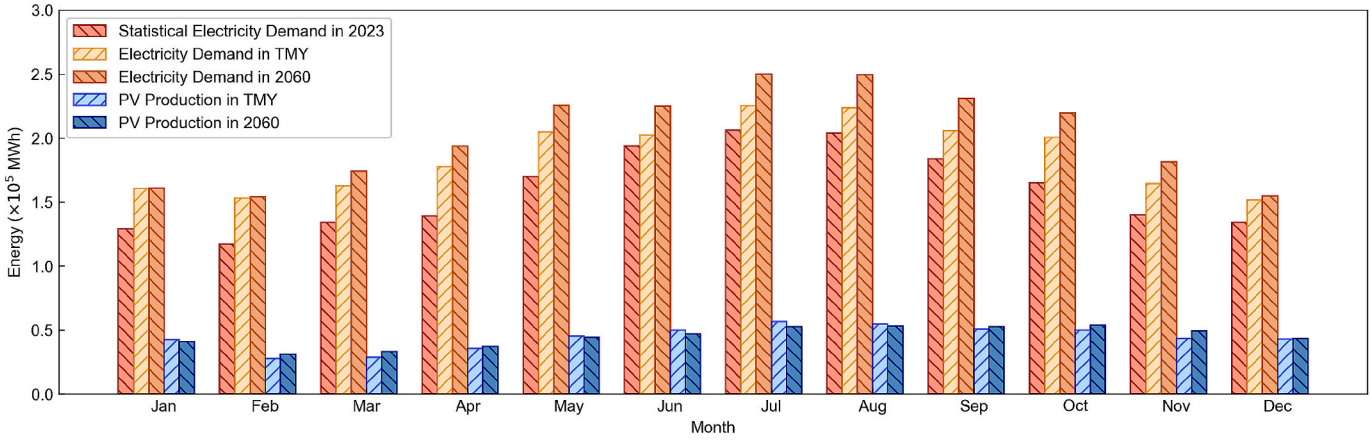

Fig. 8. Monthly electricity demand and PV production in typical year (TMY) and year 2060 (RCP 8.5).
(Note: Statistical electricity demand is from the census and statistics department in Hong Kong government [58], while other data are from the simulation results through TRNSYS [26]. This can effectively prove that simulation data from TRNSYS is reasonable.)

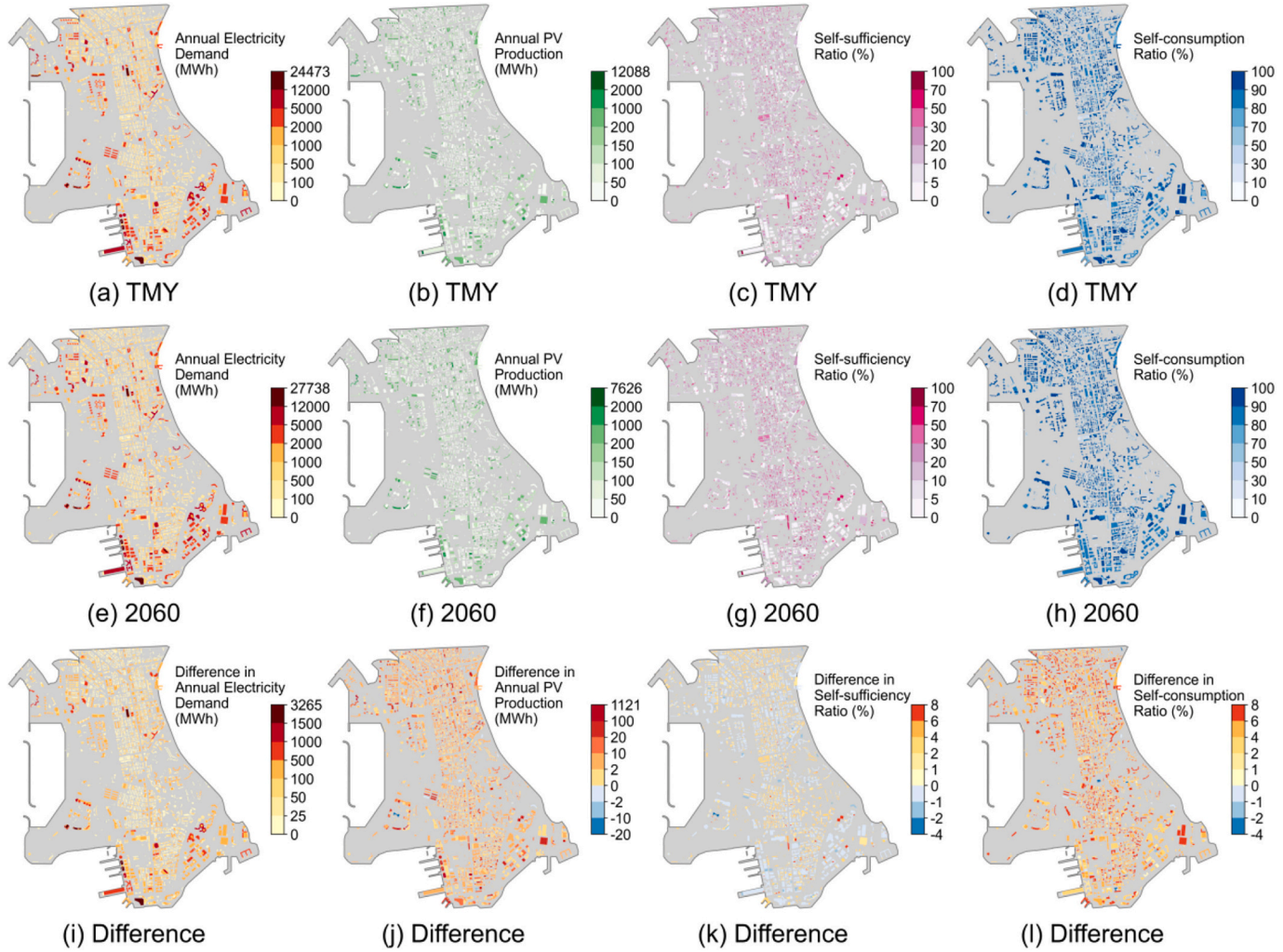

Fig. 9. Spatial distribution of PV and electricity demand: (a) annual electricity demand in TMY, (b) annual PV production in TMY, (c) self-sufficiency ratio in TMY, (d) self-consumption ratio in TMY, (e) annual electricity demand in 2060, (f) annual PV production in 2060, (g) self-sufficiency ratio in 2060, (h) self-consumption ratio in 2060, and the differences between 2060 and TMY scenarios for (i) annual electricity demand, (j) annual PV production, (k) self-sufficiency ratio, and (l) self-consumption ratio.
(Note: Self-sufficiency ratio (SSR) is defined as the proportion of the total electricity demand met by the self-consumed PV electricity, instead of being covered by grid import power. Self-consumption ratio (SCR) is defined as the proportion of the PV production that is consumed on-site to meet the electricity demand, instead of being exported to local power grid.)

assessment, economic performance of the cost and benefit of the BESS deployments requires to be evaluated by calculating the total costs, revenue, and net profits. Total cost (C_{BESS}) of the BESS refers to the total investment cost, which is calculated as

$$C_{BESS} = C_{CAPEX} \cdot TC_{BESS} \tag{18}$$

where C_{CAPEX} refers to the capital expenditure of BESS (HK$/kWh) [54] and TC_{BESS} refers to the total BESS capacity (MWh).

Revenue ($Revenue_{BESS}$) is determined based on the opportunities for energy arbitrage, where the BESS is charged during off-peak hours and discharged during peak hours no matter under normal conditions or the extreme event. It is expressed as:

$$Revenue_{BESS} = \int_{t=1}^{\text{end of lifecycle}} \left(P_{discharge}(t) \bullet Pr_{grid,peak}(t) - P_{charge}(t) \bullet Pr_{grid,off-peak}(t)\right) dt \tag{19}$$

where $P_{charge}(t)$ and $P_{discharge}(t)$ refers to the charging and discharging power at time step t, respectively. $Pr_{grid,peak}(t)$ and $Pr_{grid,off-peak}(t)$ refers to the electricity prices during peak and off-peak hours [55].

Additionally, total economic losses ($Loss_{shortage}$) during the lifecycle of BESS is incorporated into the analysis by estimating the power shortage cost associated with the total power shortage duration, which calculated as:

$$Loss_{shortage} = \int_{t=1}^{\text{end of lifecycle}} \left(P_{shortage} \cdot C_{shortage}\right) dt \tag{20}$$

where $C_{shortage}$ is the power shortage cost (HK$/kWh) [56], and $P_{shortage}$

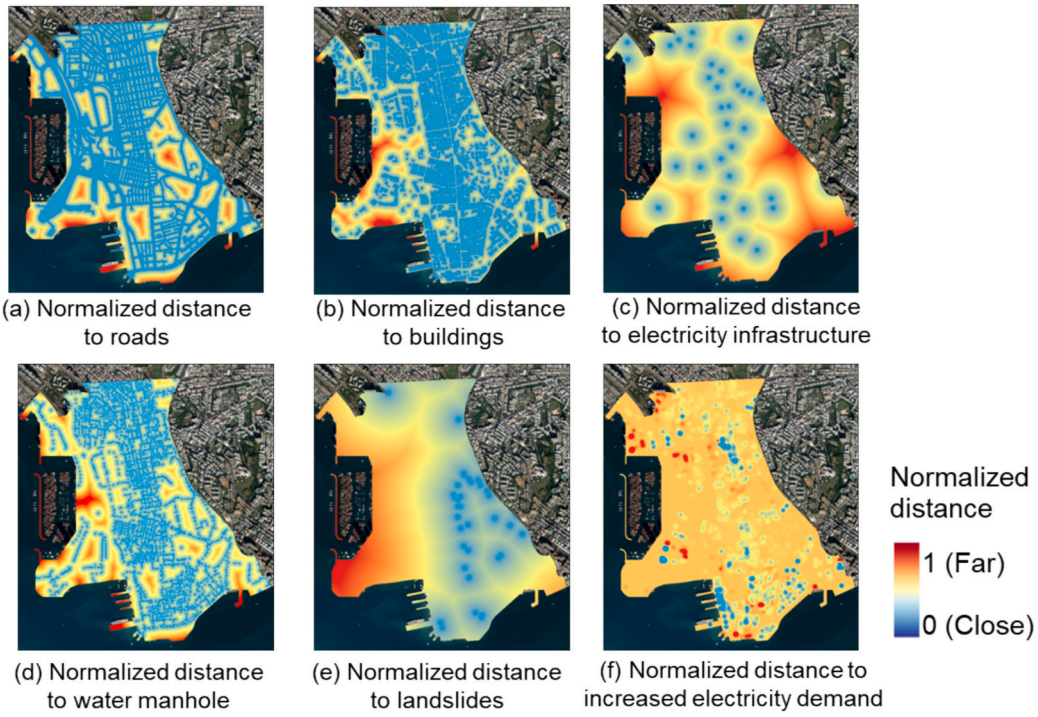

Fig. 10. Spatial distribution of the normalized distance with each criterion: (a) roads; (b) buildings; (c) electricity infrastructure; (d) water manholes; (e) landslides; (f) increased electricity demand.
(Note: Normalized distance for each criterion is formulated in Eq. (3). For criteria with roads, buildings, electricity infrastructure, water manholes and increased electricity demand (as shown in Fig. 10(a-d, f)), closer normalized distance (smaller value) demonstrates a better performance. For criteria with landslide (as shown in Fig. 10(e)), further normalized distance (larger value) demonstrates a better performance.)

is the estimated power shortage at time step t [57].

Net profit of BESS (NP_{BESS}) is defined as:

$$NP_{BESS} = R_{BESS} - C_{BESS} - Loss_{shortage} \quad (21)$$

where R_{BESS}, C_{BESS}, and $Loss_{shortage}$ are defined as the lifecycle investment cost of the BESS deployment, revenue from energy arbitrage (peak valley grid price difference), and economic losses from power shortage, and are defined in Eqs. (18–20), respectively.

3. Results and discussion

3.1. Urban energy use and PV production simulation

Fig. 8 shows the monthly electricity demand and PV production in the typical year and year 2060 (under RCP 8.5 scenario). Climate change has a greater impact on electricity demand than on PV production. For example, in July, the maximum electricity demand reaches to 2.25×10^5 MWh in the typical year, while it increases to 2.50×10^5 MWh by 10 % in 2060 under climate change. However, compared to the PV production at 5.67×10^4 MWh in July in typical year, it only decreases to 5.27×10^4 MWh by 7.1 % in 2060. The reason is that, in the subtropical climate with cooling-dominated Hong Kong [6], climate change significantly increases the cooling load and thus increases the electricity demand, while climate change has less impact on the intensity and duration of sunlight [12].

Fig. 9 shows the spatial distribution of the electricity consumption, PV production, self-sufficiency ratio and self-consumption ratio. From the overall perspective, average self-sufficiency ratio (SSR) decreases from typical year to 2060. For example, on average, SSR is 11.65 % in the typical year, while it slightly decreases to 11.33 % in 2060 (as shown in Fig. 9(c), (g)). The reason for only a slight decrease in the SSR is that although the total electricity demand increases by 1.87×10^8 MWh from TMY to 2060 (as shown in Fig. 9(i)), the increase in PV production by 5.26×10^6 MWh (as shown in Fig. 9(j)) is sufficient to maintain a relatively stable proportion of direct PV utilization against the energy demand.

However, morphological difference of buildings leads to great differences in spatial distribution of PV production and electricity demand, as well as the corresponding self-sufficiency ratio (SSR) and self-consumption ratio (SCR). For example, compared to the SSR for whole system at 11.65 % in the typical year and 11.33 % in 2060, the maximum SSR of a single building can reach to 79.79 % in the typical year (as shown in Fig. 9(c)) and 90.68 % in 2060 in some low-rise buildings (as shown in Fig. 9(g)), respectively. This highly emphasizes the differences caused by the spatial distribution of energy consumption under urban scale, resulting in significance and necessity of the optimal battery deployment from the spatial aspect to optimize overall energy efficiency and resilience of the power system.

Table 3
Weights of criteria for BESS suitability analysis.

Criteria	Quantitation	Weight
Drainage	Distance to storm water inlet	0.160
Landslide	Distance to location of landslide incidents	0.156
Proximity to demand	Distance to buildings	0.168
Proximity to infrastructure	Distance to power grid	0.156
Ease of access to roads	Distance to road network	0.173
Vulnerability of energy use	Distance to increased electricity demand	0.187

3.2. Battery energy storage system (BESS) installation location based on geographic information system with multi-criteria decision making (GIS-MCDM)

Based on the above analysis, the optimal battery deployment is significant and necessary to optimize the overall energy efficiency and resilience of the power system. Since BESS is important to balance the

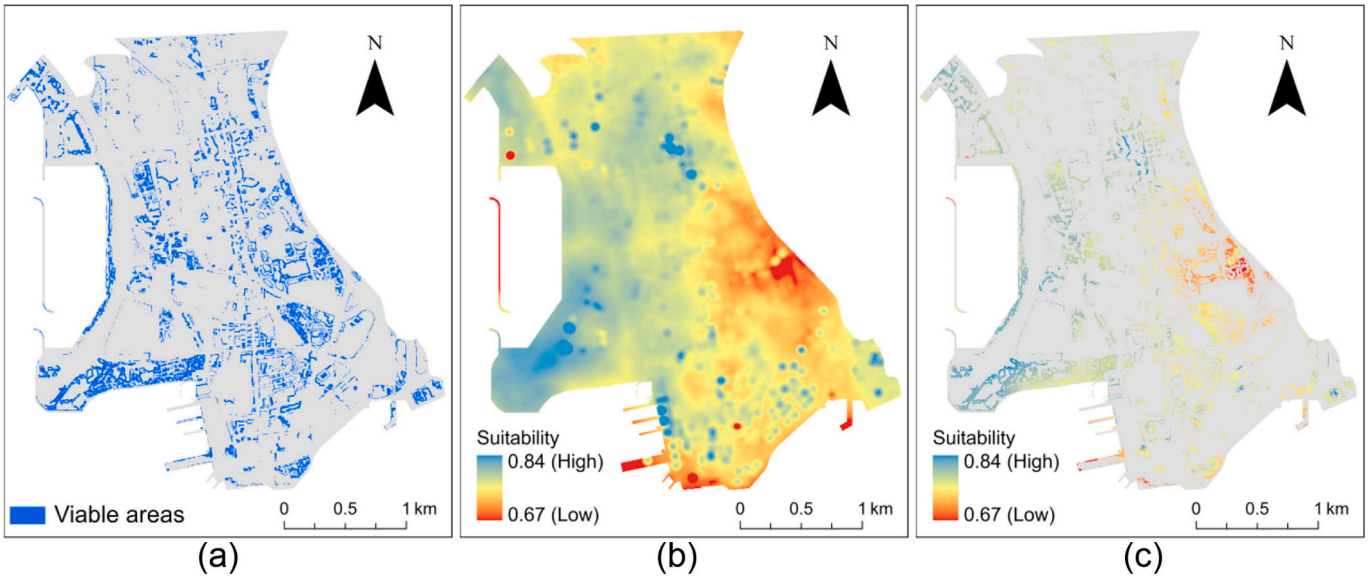

Fig. 11. (a) Feasible regions for BESS with installation conditions in reality; (b) Composite weighted suitability of BESS installation; (c) Feasible regions with suitability scores for BESS installation under urban scale.
(Note: Feasible regions for BESS are selected through feasible installation criteria (as shown in Table 1), which excludes regions with restricted geographical areas. Composite weighted suitability is calculated from the individual suitability (as shown in Fig. 10) using entropy weight (as shown in Table 3). Practical regions with high suitability are defined as the overlapped regions between feasible regions and high suitability regions, and the following optimal BESS deployment are selected from those regions.)

spatiotemporal mismatch between renewable supply and electricity demand in Hong Kong, practical installation conditions for large-scale battery deployment need to be considered under urban scale in reality. High quality installation locations are required to be selected following multi-criteria. In the GIS-MCDM approach, multiple spatial criteria are derived from the raw GIS data based on the specific factors (Table 1 and Table 2). These criteria include geographical conditions (such as slope and land use), accessibility, and safety measures. The process begins with the collection of raw GIS data layers, which provide foundational geographic information of each criterion. The criteria used for the analysis are then derived and selected based on their relevance to the study (Table 2). These criteria are weighted using the entropy weight method to reflect their relative importance in the local context of the Yau Tsim Mong district. After filtering the initial possible locations based on exclusion criteria (Table 1), the weighted criteria are overlaid to generate a suitability score map, which identifies the most suitable locations for BESS deployment.

Fig. 10 shows the spatially suitable distribution of BESS based on each criterion as proposed in Table 2. From the perspective of flexibility and accessibility, most regions are suitable for BESS installation. However, from the perspective of safety and resilience, regions that are suitable for BESS installation significantly decreases. For example, as shown in Fig. 10(a)-(d), most regions are close to roads, buildings, and electricity infrastructure with high flexibility and accessibility, which are suitable for BESS installation. The reason is that, highly densified buildings and well-established road networks in Hong Kong provide

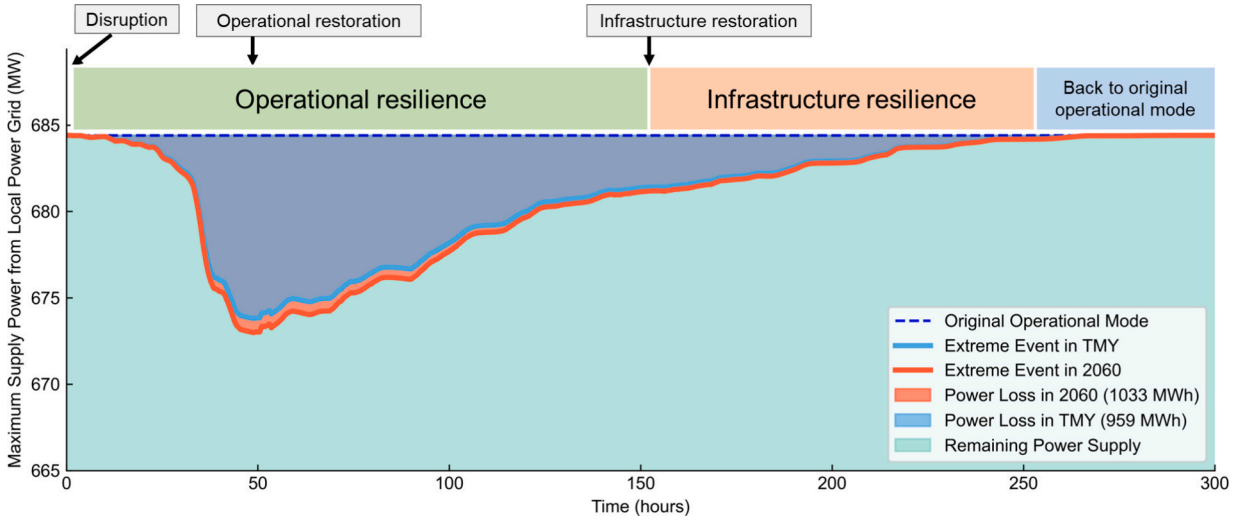

Fig. 12. Impact of extreme weather event on the maximum supply power from local power grid in typical year and 2060.
(Note: The maximum supply capacity under the original operational mode is defined as the maximum electricity demand at 684 MW in the typical year. Power loss refers to the decreased power supply from local power grid due to the extreme weather events. More detailed description for the simulated power outage can be found in Methodology.)

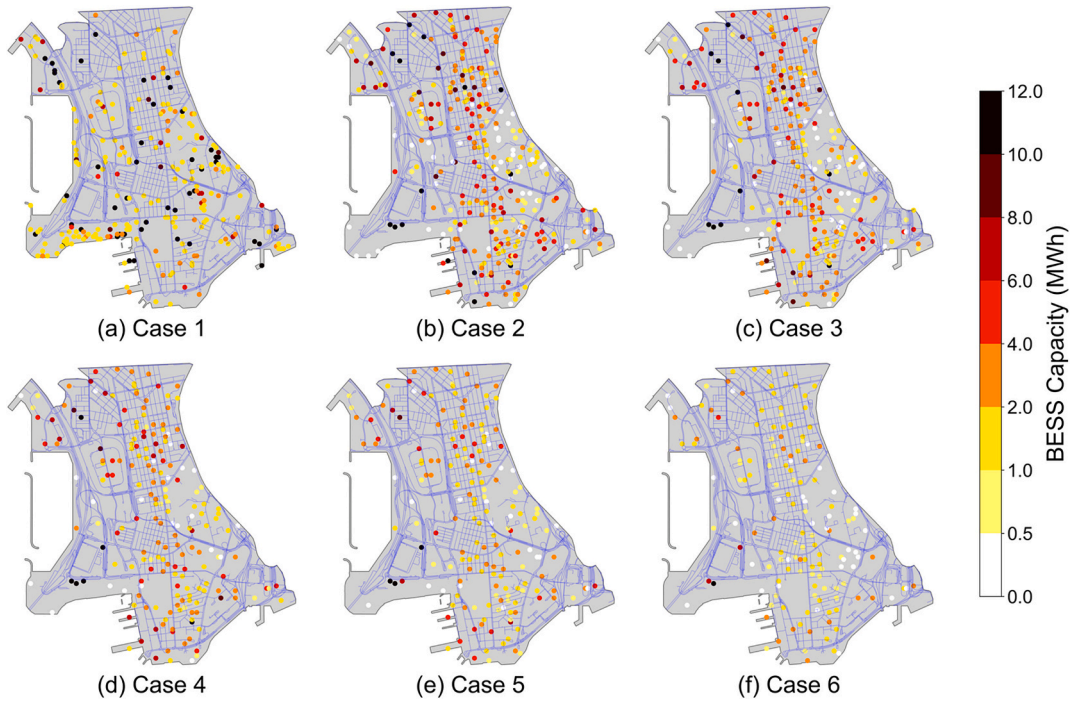

Fig. 13. Spatial distribution and capacity allocation of the BESS deployment:
(a) Case 1 (1033 MWh BESS without GIS-MCDM method);
(b) Case 2 (Optimal case: 1033 MWh BESS with GIS-MCDM method);
(c) Case 3 (800 MWh BESS with GIS-MCDM method);
(d) Case 4 (600 MWh BESS with GIS-MCDM method);
(e) Case 5 (400 MWh BESS with GIS-MCDM method);
(f) Case 6 (200 MWh BESS with GIS-MCDM method).

excellent infrastructures to support geographical conditions for BESS installations. However, as shown in Fig. 10(e)-(f), considering the safety of topographic condition and resilience, BESS installation locations are strictly restricted in regions far from landslides and close to incremental cooling loads, resulting in fewer suitable areas. The reason for the landslide is that Hong Kong's terrain is marked by steep slopes and hilly areas, while higher magnitude of the increased cooling load is due to the concentration of high-density buildings in that area.

The weight distribution for the multi-criteria decision-making process is determined using the entropy method, which objectively assigns weights based on the variability of each criterion across the study area. As shown in Table 3 and Fig. 10, the criteria with higher variability have higher weights, indicating their greater influence on the BESS installation location decision-making process. For example, the vulnerability of energy use criterion reaches the highest weight at 0.187. This criterion measures the proximity to high-demand areas, which exhibited

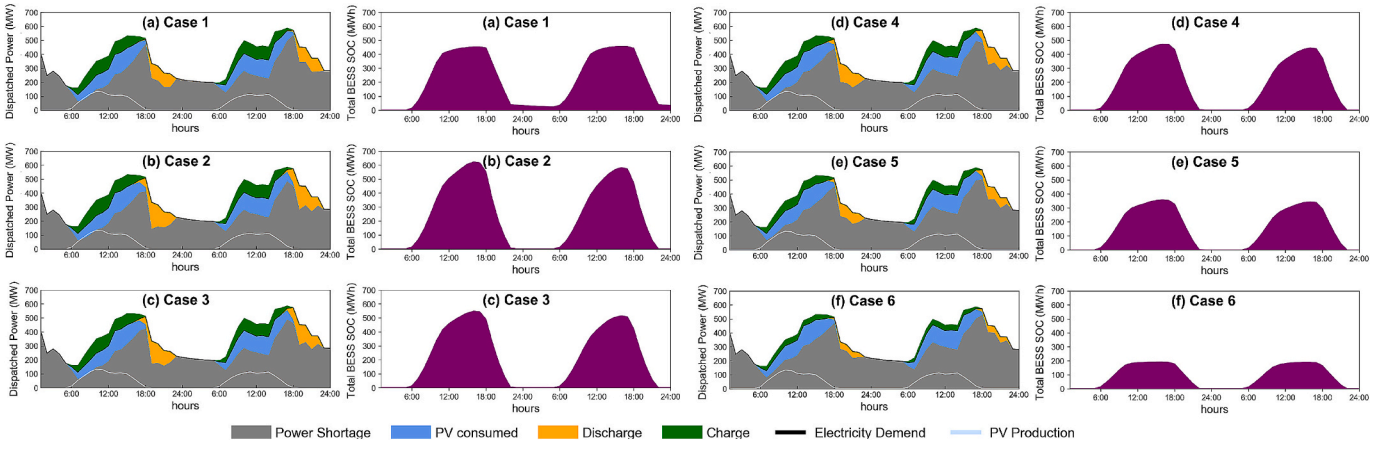

Fig. 14. Hourly dispatch sources and stage of charge of total BESS during 2-day extreme weather event under:
(a) Case 1 (1033 MWh BESS without GIS-MCDM method);
(b) Case 2 (Optimal case: 1033 MWh BESS with GIS-MCDM method);
(c) Case 3 (800 MWh BESS with GIS-MCDM method);
(d) Case 4 (600 MWh BESS with GIS-MCDM method);
(e) Case 5 (400 MWh BESS with GIS-MCDM method);
(f) Case 6 (200 MWh BESS with GIS-MCDM method).

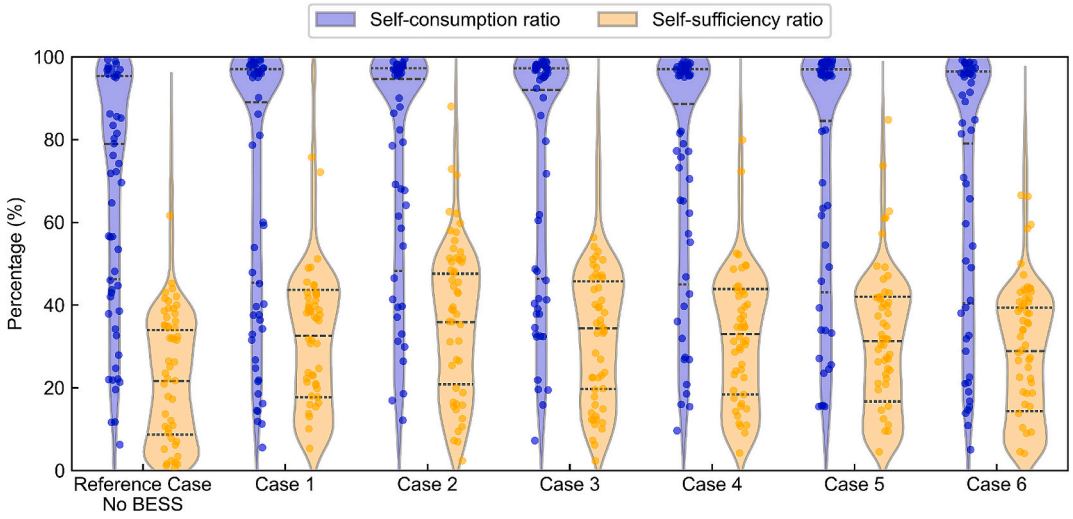

Fig. 15. Violin plot for annual self-consumption ratio (SCR) and self-sufficiency ratio (SSR) in different scenarios.
(Note: Three dashed lines in the violin plot from top to bottom represent the 75th percentile (upper quartile), the median (50th percentile), and the 25th percentile (lower quartile). Case 1–6 in Fig. 15 corresponds to the cases listed in Table 4.) As for self-consumption ratio (SCR) and self-sufficiency ratio (SSR), optimal BESS deployment with GIS-MCDM method is more advantageous in terms of both SCR and SSR with a better overall performance. For example, regarding the SSR, compared to the Case 1 with the maximum SSR at 90.68 %, optimal BESS deployment increases the maximum SSR to 97.11 %. Moreover, distribution of SSR under optimal BESS deployment demonstrates more stable. Regarding the SCR, optimal BESS deployment shows that the maximum SCR reaches to 99.50 %, which is a little bite larger than the other scenarios. Therefore, optimal BESS deployment not only maximizes the utilization of renewable energy sources, but also improves the resilience and reliability of the power supply during extreme weather events, making it a vital strategy for sustainable energy management.

substantial variation across the region (as shown in Fig. 10(f)). The high demand areas are crucial for ensuring energy resilience, particularly during extreme weather events, as they are most susceptible to power shortages [48]. Prioritizing these regions ensures the optimal placement of BESS to enhance the system's emergency response capacity and reduce disruptions, aligning with the study's goal of improving urban energy resilience.

Moreover, ease of access to roads is assigned the second-highest weight at 0.173, reflecting the considerable variability in road accessibility across the study area, as seen in Fig. 10(a). Locations with better access to roads are preferred for BESS deployment because they reduce installation and maintenance costs, enhancing the long-term feasibility of the project. Urban regions with dense infrastructure benefit from better road networks, which simplifies logistics and operational efficiency [49,50]. On the other hand, criterion like landslide risk has a relatively lower weight at 0.156, as its spatial variation is less significant (as shown Fig. 10(e)). While landslide risk is an important safety consideration, fewer regions in the study area are significantly affected, reducing its overall impact on the BESS deployment. These weight distributions underscore the importance of prioritizing criteria that exhibit greater spatial variability, as they provide more meaningful contributions to the optimization process. Criteria that show greater spatial differences, such as energy demand vulnerability and road accessibility, are assigned to higher weights, as their variability has a larger influence on the spatial distribution of the BESS.

Fig. 11 shows the suitable regions for BESS installation. Considering combined effects of feasible regions with high suitability, central and southern regions show higher suitability for BESS installation, while the northern and peripheral regions display lower suitability. This can be indicated by the distribution of feasible regions for BESS in Fig. 11(a). The higher suitability in the central and southern regions can be attributed to the availability of vacant spaces and fewer structural obstacles, as well as their proximity to major transportation and commercial hubs, which facilitate BESS installation due to higher electricity demands and better infrastructure support. Conversely, the lower suitability in the northern and peripheral regions is due to higher building density, less available space, and higher risk of landslides, which can pose challenges to BESS installation. Overall, intricate balance for BESS installation locations under multi-criteria highlights the necessity for considering the real-world condition under the urban-scale.

Table 4
Cases for BESS deployment in different capacities with and without GIS-MCDM method.

Cases	Total BESS capacity (MWh)	Maximum limit of charging/discharging power (MW) [60]	Location siting and capacity sizing of BESS approaches
Reference	0	0	\
Case 1	1033	258.25	Random selection (without GIS-MCDM method)
Case 2 (Optimal)	1033	258.25	GIS-MCDM method
Case 3	800	200	GIS-MCDM method
Case 4	600	150	GIS-MCDM method
Case 5	400	100	GIS-MCDM method
Case 6	200	50	GIS-MCDM method

3.3. BESS deployment and performance analysis

Under climate change and extreme weather events, power supply from the local grid becomes unstable. Power outages simulation under extreme weather events is necessary for subsequent optimal BESS deployment to enhance energy resilience. Fig. 12 shows the maximum supply power from the local power grid under extreme weather events across different scenarios. Extreme weather events at the current stage can significantly decrease the energy resilience of the power system, while extreme weather events in 2060 will further reduce energy resilience. For example, compared to the original mode at 684 MW, the maximum power supplied from local power grid decreases to 673 MW in 2060 under extreme weather events. This is due to the increased frequency and intensity of extreme weather events in the future [59]. Based on above, total capacity of the BESS is defined as the total loss energy under extreme weather events in 2060 at 1033 MWh (as shown in Fig. 12).

Following the GIS-MCDM method (as introduced in Methodology), the spatial distribution and capacity allocation of BESS in Yau Tsim

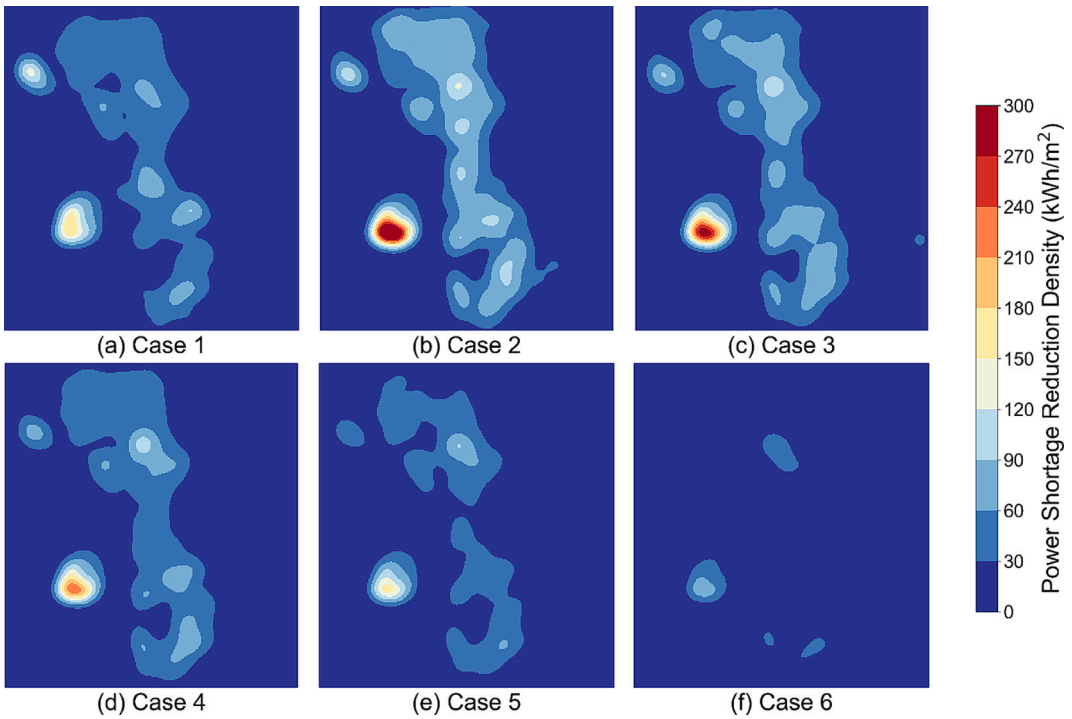

Fig. 16. Power shortage reduction density and power shortage reduction under different scenarios:
(a) Case 1 (1033 MWh BESS without GIS-MCDM method);
(b) Case 2 (optimal case: 1033 MWh BESS with GIS-MCDM method);
(c) Case 3 (800 MWh BESS with GIS-MCDM method);
(d) Case 4 (600 MWh BESS with GIS-MCDM method);
(e) Case 5 (400 MWh BESS with GIS-MCDM method);
(f) Case 6 (200 MWh BESS with GIS-MCDM method).

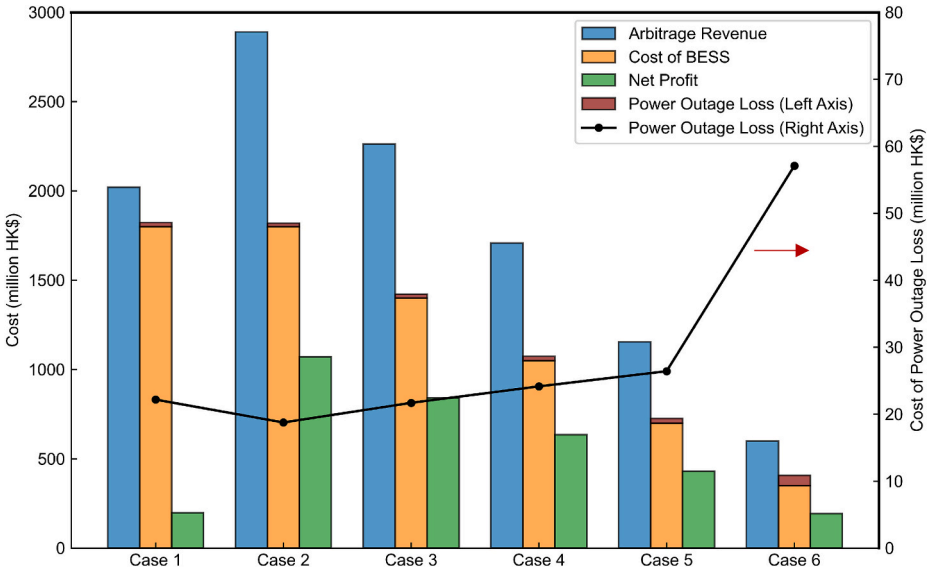

Fig. 17. Economic performance of different BESS deployments from Case 1 to Case 6.

Mong are demonstrated in Fig. 13(b). Meanwhile, Case 1 is designed with the same battery capacity (1033 MWh) without optimal location selection. Furthermore, BESS capacities from 200 MWh to 800 MWh with a resolution of 200 MWh following the GIS-MCDM method are also designed for comparative analysis. Clearly, BESS with optimal location and capacity deployment leads to the sufficient usage of BESS to avoid regions with low electricity demand and oversized BESS installation. For example, compared to the Case 1 with a scattered distribution with high-capacity allocation (as shown in Fig. 13(a)), BESS with optimal deployment (as shown in Fig. 13(b)) concentrates more in regions with high electricity demand and achieves a more uniform distribution.

In order to demonstrate the effectiveness of the proposed GIS-MCDM method on BESS deployment, Fig. 14 shows the performance evaluation of the deployed BESS with the GIS-MCDM method during a 2-day power outage event. Notable performance improvement can be achieved through the proposed GIS-MCMD method in optimizing capacity

allocation and installation locations for BESS deployment. Even with the same battery capacity, the GIS-MCMD method in optimizing capacity allocation and installation locations for BESS deployment can effectively reduce severe power outages. For example, even with the same BESS capacity at 1033 MWh, compared to the power shortage at 13184 MWh in Case 1 (1033 MWh BESS without GIS-MCDM method, as shown in Fig. 14(a)), optimal BESS deployment decreases the power shortage to 12,931 MWh (as shown in Fig. 14(b)). This is due to the improved spatial distribution of BESS, which ensures that areas with higher electricity demand receive adequate storage capacity, thereby enhancing the overall efficiency and resilience of the power system.

Moreover, higher battery capacities and optimal location selection significantly mitigate the severity of power shortages. For instance, compared to the BESS at 200 MWh in Case 6, optimal BESS deployment in Case 2 decreases the power shortage from 14,159 MWh to 12,931 MWh (as shown in Fig. 14(b), (f)), leading to 8.7 % mitigation of the power shortage. The reason is that larger battery capacity can provide a greater buffer to store excess energy, thereby significantly reducing the occurrence and severity of power shortages. Overall, sufficient capacity combined with optimal installation and strategic allocation is crucial for enhancing energy resilience and resisting unexpected disruptions.

For the performance evaluation from the spatial aspects, Fig. 16 shows the density power outage reduced by PV-BESS system to evaluate to evaluate the effectiveness of BESS deployment in mitigating power shortages across various regions. Clearly, the higher BESS capacity and optimal deployments can effectively reduce the incidence and severity of power shortages, particularly in high-demand areas, thus enhancing the overall resilience of the power system. For example, compared to BESS without GIS-MCDM (Case 1) with maximum power shortage reduction density at 176.04 kWh/m^2 and the area of power shortage reduction density above 100kWh/m^2 at 1.24 $\times$ 10^5 m^2 (as shown in Fig. 16(a)), optimal BESS deployment (as shown in Fig. 16(b)) increases the maximum power shortage reduction density to 364.2 kWh/m^2 and increases the area of power shortage reduction density above 100kWh/m^2 to 2.17 $\times$ 10^5 m^2. The colour in Fig. 16(b) shows significantly redder areas, indicating a larger magnitude of power shortage reduction. This region in reality corresponds to the zone around the International Commerce Centre, which includes high density high-rise buildings with higher energy consumption, while optimal BESS deployment is more focused on regions with higher electricity demand density, leading to larger power shortage reduction. Areas with high building density and electricity demand will experience greater power shortage during outages. Prioritizing energy storage resources in these locations can effectively reduce power shortage density, offering crucial insights for future planning. Therefore, optimized BESS deployment in these high-demand areas leads to a significant reduction in power shortages. Furthermore, the decrease in BESS deployment capacity reduces the power shortage reduction ability, as indicated by the less densified distribution in Fig. 16 (c-f) with lighter colour. Overall, these findings significantly emphasize the critical role of adequate BESS capacity and strategic location deployment in reducing power shortage impacts and increasing the energy resilience under urban scale.

To further assess the economic performance of BESS with different capacities in Case 1 to 6, lifecycle costs of BESS, net profit, and power shortage-related economic losses have been calculated to provide a comprehensive comparison of the financial feasibility and impact of each scenario. BESS deployment with optimal capacity allocation and installation selection contributes to more net profits. For example, as shown in Fig. 17, compared to the BESS capacity at 1033 MWh in Case 1 with the net profit at 217.37 million HK$, optimal BESS deployment with BESS capacity at 1033 MWh in Case 2 shows a higher net profit at 1087.91 million HK$. The reason is that the optimal BESS deployment in Case 2 ensures that the storage capacity is effectively aligned with buildings that have significant energy demands. This optimal alignment allows for a better match between the BESS discharge capabilities and local consumption patterns, leading to higher utilization rates of the stored energy. As a result, the BESS in Case 2 can participate more efficiently in peak shaving and energy arbitrage activities, thereby generating higher revenue compared to the randomly sited BESS in Case 1.

Furthermore, as the capacity of BESS decreases, economic loss for power shortage gradually increases and net profit of BESS gradually decreases. For example, BESS capacity at 200 MWh in Case 6 shows the lowest net profit at 244.51 million HK$ with the highest power shortage related loss at 57.08 million HK$, while BESS capacity at 1033 MWh in Case 2 shows the highest net profit at 1087.91 million HK$ with the lowest power shortage related loss at 18.75 million HK$. The reason is that, BESS with higher capacity shows higher energy resilience for power shortage reduction during extreme events periods, and higher cost-effectiveness for energy arbitrage during the normal conditions, leading to lower economic losses and higher net profits. These findings highlight the need to carefully balance the investment in BESS capacity with energy resilience and economic returns. Optimal BESS deployment with a larger battery capacity offers a dual advantage, i.e., they not only deliver higher profits, but also ensure higher energy resilience by effectively mitigating power outage losses. However, it is worth noting that the high revenue of high-capacity BESS is based on the premise that the BESS can fully participate in electricity market arbitrage to obtain profit from peak and off-peak grid price difference. Intermediate capacities, such as 800 MWh in Case 3 and 600 MWh in Case 4, may provide a cost-effective alternative, striking a balance between cost and performance, without significantly compromising the ability to mitigate power shortage related losses.

3.4. Research limitations and future outlook

This research provides a complete method for the optimal BESS deployment under extreme events to improve the energy resilience of the power system. By systematically analysing optimal locations and appropriate capacity distribution, energy resilience of the power system can be significantly increased during extreme events, ensuring reliable energy supply and reducing the severe impact of disruptions. While the methodology in this study was developed and tested using data from Hong Kong, its framework is designed to be highly adaptable to other regions. The GIS data utilized in this study, including road networks, land use, digital elevation models (DEMs), and detailed regional power infrastructure, were sourced from open-source projects, ensuring that the same methodology can be applied to various urban areas worldwide. Furthermore, the power flow simulations conducted in this study were carried out using the open-source PyPSA model [52]. The approach can be adapted by adjusting local parameters, such as energy demand, grid characteristics and constraints, while retaining the core framework. The BESS deployment framework, the resilience metrics and the KDE of power shortage reductions are suited for urban areas vulnerable to grid disruptions caused by extreme weather or other factors. However, some limitations should be noted:

(1) Optimal economic costs and environmental impacts associated with the implementation of the BESS deployment are not taken into account. This may result in overlooking significant financial burdens and potential environmental pollutions, which could render the BESS deployment to be impractical or unsustainable in real-world applications.
(2) Resilience assessment for the proposed BESS deployment is limited to short-term extreme events and does not consider long-term deployment scenarios. This limitation fails to address the potential degradation and long-term performance issues of the PV-BESS system, which may compromise its effectiveness and reliability over long-term operation.
(3) Method for determining the total capacity of BESS is relatively simplified and rough, which may not capture the accurate requirement for the total BESS capacity under the long-term

operation. This may result in either under-sizing with compromised reliability, or over-sizing with unnecessary costs and inefficiencies.
(4) The BESS deployment method proposed in this research are constrained by the dynamic nature of urban development and climate change. As cities and environmental conditions evolve at an accelerating pace, these factors may limit the scalability of the BESS deployment and diminish its long-term effectiveness.

Based on the above limitations, future research will focus on:

(1) Detailed cost-benefit analyses and environmental impact assessments should be integrated into the proposed optimal BESS deployment method. This will enable a holistic evaluation of the proposed energy resilience strategies, ensuring they are technically viable, economically feasible, and environmentally sustainable.
(2) Long-term performance and sustainability of the PV-BESS system should be further considered, which will ensure the energy resilience strategies remain effective over extended periods and under varying environmental conditions.
(3) Methodology should be refined for determining the optimal total BESS capacity, considering the dynamic behaviour of electricity demand and supply in a long-term operation. This refinement will ensure a more precise and effective BESS deployment, enhancing the overall resilience and efficiency of the power system.
(4) Integration of real-time data and adaptive learning mechanisms should be considered to further enhance the flexibility and responsiveness of the BESS deployment strategy. Real-time data, such as live energy consumption, weather forecasts, and grid conditions, could be integrated into the model to allow for dynamic adjustments in BESS locations and capacities in response to immediate changes in urban conditions. Additionally, implementing adaptive learning mechanisms, such as machine learning algorithms, would enable the system to continuously refine and optimize deployment strategies based on historical data and evolving trends. This could improve both the short-term effectiveness and the long-term adaptability of the system, ensuring that BESS deployment remains robust and scalable across diverse urban settings.

4. Conclusion

In this research, battery energy storage system (BESS) deployment under urban scale has been fully developed to enhance the energy resilience of the power system under future climate change and extreme weather events. A geographic information system with multi-criteria decision making (GIS-MCDM) approach has been proposed to identify the feasible BESS installation locations under the urban scale, considering practical geographical conditions and the proposed energy resilience criterion (i.e., distance to the increased electricity demand). Furthermore, BESS deployment based on the Capacitated P-Median Problem (CPMP) has been provided with the optimal and specific installation location and capacity allocation under extreme events. Last but not the least, performance of the proposed optimal BESS deployment has been thoroughly evaluated from multi-aspects to improve the effectiveness on enhancing urban energy resilience and maintaining the stability of the power system. Main conclusions are shown below:

(1) A comprehensive framework for BESS deployment under urban scale has been proposed to enhance the energy resilience of the power system. Suitable installation locations can be firstly identified based on the proposed GIS-MCDM method. It has been found that central and southern regions in Yau Tsim Mong show higher suitability for BESS installation, while the northern and peripheral regions display lower suitability.
(2) BESS deployment based on the Capacitated P-Median Problem (CPMP) has been provided with optimal and specific installation location and capacity allocation under extreme weather events. Compared to the BESS without optimal deployment, BESS with optimal deployment is mainly distributed in regions with high electricity demands and achieves a more uniform distribution with better performances.
(3) Performance of the proposed optimal BESS deployment approach has been analysed and validated to be superior to other approaches from both temporal and spatial aspects. From the temporal aspect, the optimal BESS deployment in Case 2 decreases the power shortage from 14,159 MWh to 12,931 MWh by 8.7 %. From the spatial aspect, compared to the BESS deployment without GIS-MCDM, the optimal BESS deployment increases the maximum power shortage reduction density from 176.04 to 364.2 kWh/m^2 and increases the area of power shortage reduction density above 100 kWh/m^2 from 1.24×10^5 to 2.17×10^5 m^2 by 75 %. Moreover, compared to the BESS capacity at 1033 MWh in Case 1 with the net profit at 217.37 million HK$, BESS deployment with BESS capacity at 1033 MWh in Case 2 demonstrates better economic performance, with a higher net profit at 1087.91 million HK$.

In addition to the findings specific to Hong Kong, this study has broader implications for enhancing urban energy resilience globally. The GIS-MCDM approach proposed in this research offers a flexible and scalable framework that can be adapted to other cities facing similar energy challenges, such as increased demand, renewable energy integration, and vulnerability to extreme events. Cities with diverse geographic, infrastructural, and environmental conditions can benefit from this method by tailoring the criteria and weighting factors to their unique circumstances. By adopting this approach, cities worldwide can optimize their BESS deployment strategies, improving both energy resilience and sustainability in the face of growing climate risks and urbanization pressures. Future studies can work on hydrogen-driven city-scale energy resilience under climate change, like carbon footprint quantificaation [61] and climate change adaptation [62] so on.

Overall, this research significantly highlights the importance of BESS deployment on an urban scale, providing frontier guidelines on system designers and urban planners to collaboratively develop a reliable power system with high energy resilience.

CRediT authorship contribution statement

Dazhou Ping: Writing – review & editing, Writing – original draft, Methodology, Investigation, Conceptualization. **Chaosu Li:** Writing – review & editing, Writing – original draft, Supervision, Methodology, Investigation, Funding acquisition, Conceptualization. **Xiaojun Yu:** Methodology, Investigation, Data curation. **Zhengxuan Liu:** Methodology, Investigation, Data curation. **Ran Tu:** Methodology, Investigation, Formal analysis, Conceptualization. **Yuekuan Zhou:** Writing – review & editing, Writing – original draft, Validation, Supervision, Resources, Project administration, Methodology, Investigation, Funding acquisition, Data curation, Conceptualization.

Declaration of competing interest

The authors declare that they have no known competing financial interests or personal relationships that could have appeared to influence the work reported in this paper.

Data availability

The data that has been used is confidential.

Acknowledgement

This work was supported by National Natural Science Foundation of China (NSFC) (52408137, 52378079), Guangdong Provincial Natural Science Foundation General Project (2414050003253, 2024A1515011609), Guangdong Province Joint Fund for Basic and Applied Basic Research (2022A1515110364, 2023A04J1035), Municipal University (Institute) Enterprise Joint Funding Project (2023A03J0104), Yangcheng Scholars Leading Talent Training Project (2024312133), HKUST(GZ)-enterprise cooperation projects (R00017-2001, R00072-2001, R00079-2001). This research is also supported by The Hong Kong University of Science and Technology (Guangzhou) startup grant (G0101000059), Project of Hetao Shenzhen-Hong Kong Science and Technology Innovation Cooperation Zone (HZQB-KCZYB-2020083) and Special Project of Joint Funding from Municipal Schools (Institutes) and Enterprises-Basic Research Program (2024A03J0630).

Appendix A. Supplementary data

Supplementary data to this article can be found online at https://doi.org/10.1016/j.apenergy.2024.124813.

References

[1] Gernaat DEHJ, de Boer HS, Daioglou V, Yalew SG, Müller C, van Vuuren DP. Climate change impacts on renewable energy supply. Nat Clim Chang 2021;11:119–25. https://doi.org/10.1038/s41558-020-00949-9.
[2] Sharifi A, Yamagata Y. Principles and criteria for assessing urban energy resilience: a literature review. Renew Sust Energ Rev 2016;60:1654–77. https://doi.org/10.1016/j.rser.2016.03.028.
[3] Erker S, Stangl R, Stoeglehner G. Resilience in the light of energy crises – part I: a framework to conceptualise regional energy resilience. J Clean Prod 2017;164:420–33. https://doi.org/10.1016/j.jclepro.2017.06.163.
[4] Jasiūnas J, Lund PD, Mikkola J. Energy system resilience – a review. Renew Sust Energ Rev 2021;150:111476. https://doi.org/10.1016/j.rser.2021.111476.
[5] Xu L, Feng K, Lin N, Perera ATD, Poor HV, Xie L, et al. Resilience of renewable power systems under climate risks. Nat Rev Electr Eng 2024;1:53–66. https://doi.org/10.1038/s44287-023-00003-8.
[6] Zhou Y, Dan Z, Yu X. Climate-adaptive resilience in district buildings and cross-regional energy sharing in Guangzhou-Shenzhen-Hong Kong Greater Bay Area. Energ Buildings 2024;308:114004. https://doi.org/10.1016/j.enbuild.2024.114004.
[7] Mishra DK, Ghadi MJ, Azizivahed A, Li L, Zhang J. A review on resilience studies in active distribution systems. Renew Sust Energ Rev 2021;135:110201. https://doi.org/10.1016/j.rser.2020.110201.
[8] Moazami A, Nik VM, Carlucci S, Geving S. Impacts of future weather data typology on building energy performance – investigating long-term patterns of climate change and extreme weather conditions. Appl Energy 2019;238:696–720. https://doi.org/10.1016/j.apenergy.2019.01.085.
[9] Berardi U, Jafarpur P. Assessing the impact of climate change on building heating and cooling energy demand in Canada. Renew Sust Energ Rev 2020;121:109681. https://doi.org/10.1016/j.rser.2019.109681.
[10] Flores-Larsen S, Filippín C, Barea G. Impact of climate change on energy use and bioclimatic design of residential buildings in the 21st century in Argentina. Energ Buildings 2019;184:216–29. https://doi.org/10.1016/j.enbuild.2018.12.015.
[11] Feron S, Cordero RR, Damiani A, Jackson RB. Climate change extremes and photovoltaic power output. Nat Sustain 2021;4:270–6. https://doi.org/10.1038/s41893-020-00643-w.
[12] Zhao X, Huang G, Lu C, Zhou X, Li Y. Impacts of climate change on photovoltaic energy potential: a case study of China. Appl Energy 2020;280:115888. https://doi.org/10.1016/j.apenergy.2020.115888.
[13] Peng L, Mauzerall DL, Zhong YD, He G. Heterogeneous effects of battery storage deployment strategies on decarbonization of provincial power systems in China. Nat Commun 2023;14:4858. https://doi.org/10.1038/s41467-023-40337-3.
[14] Li Y, Wei Y, Zhu F, Du J, Zhao Z, Ouyang M. The path enabling storage of renewable energy toward carbon neutralization in China. eTransportation 2023;16:100226. https://doi.org/10.1016/j.etran.2023.100226.
[15] He G, Lin J, Sifuentes F, Liu X, Abhyankar N, Phadke A. Rapid cost decrease of renewables and storage accelerates the decarbonization of China's power system. Nat Commun 2020;11:2486. https://doi.org/10.1038/s41467-020-16184-x.
[16] Liu H, Brown T, Andresen GB, Schlachtberger DP, Greiner M. The role of hydro power, storage and transmission in the decarbonization of the Chinese power system. Appl Energy 2019;239:1308–21. https://doi.org/10.1016/j.apenergy.2019.02.009.
[17] Uncertainty-aware deployment of mobile energy storage systems for distribution grid resilience | ieee journals & magazine | ieee xplore. https://ieeexplore.ieee.org/abstract/document/9372331. [Accessed 10 June 2024].
[18] Rajabzadeh M, Kalantar M. Enhance the resilience of distribution system against direct and indirect effects of extreme winds using battery energy storage systems. Sustain Cities Soc 2022;76:103486. https://doi.org/10.1016/j.scs.2021.103486.
[19] Palmer JF. The contribution of a GIS-based landscape assessment model to a scientifically rigorous approach to visual impact assessment. Landsc Urban Plan 2019;189:80–90. https://doi.org/10.1016/j.landurbplan.2019.03.005.
[20] Divu DN, Mojjada SK, Pokkathappada AA, Sukhdhane K, Menon M, Mojjada RK, et al. Decision-making framework for identifying best suitable mariculture sites along north east coast of Arabian Sea, India: a preliminary GIS-MCE based modelling approach. J Clean Prod 2021;284:124760. https://doi.org/10.1016/j.jclepro.2020.124760.
[21] Huang W, Ling M. System resilience assessment method of urban lifeline system for GIS. Comput Environ Urban Syst 2018;71:67–80. https://doi.org/10.1016/j.compenvurbsys.2018.04.003.
[22] Alhamwi A, Medjroubi W, Vogt T, Agert C. Development of a GIS-based platform for the allocation and optimisation of distributed storage in urban energy systems. Appl Energy 2019;251:113360. https://doi.org/10.1016/j.apenergy.2019.113360.
[23] Wei T, Zhang Y, Zhang Y, Miao R, Kang J, Qi H. City-scale roof-top photovoltaic deployment planning. Appl Energy 2024;368:123461. https://doi.org/10.1016/j.apenergy.2024.123461.
[24] Optimal deployment of distributed rooftop photovoltaic systems and batteries for achieving net-zero energy of electric bus transportation in high-density cities. Appl Energy 2022;319:119274. https://doi.org/10.1016/j.apenergy.2022.119274.
[25] Zhou J, Wu Y, Wu C, He F, Zhang B, Liu F. A geographical information system based multi-criteria decision-making approach for location analysis and evaluation of urban photovoltaic charging station: a case study in Beijing. Energy Convers Manag 2020;205:112340. https://doi.org/10.1016/j.enconman.2019.112340.
[26] WELCOME | TRNSYS : transient system simulation tool. https://www.trnsys.com/. [Accessed 20 June 2024].
[27] Design code for residential buildings. GB 50096–2011, https://www.mohurd.gov.cn/gongkai/fdzdgknr/tzgg/201110/20111026_206878.html; 2011.
[28] Standard for design of office building. JGJ/T67–2019, http://www.gov.cn/zhengce/zhengceku/2020-04/03/content_5498866.htm; 2019.
[29] Code for design of hotel building. JGJ62–2014, https://www.mohurd.gov.cn/gongkai/fdzdgknr/tzgg/201409/20140902_224213.html; 2014.
[30] Meteonorm. Meteonorm. Retrieved from: https://meteonorm.com/; 2003.
[31] Amap. https://ditu.amap.com/; 2024. accessed June 20, 2024.
[32] Biljecki F, Ledoux H, Stoter J. An improved LOD specification for 3D building models. Comput Environ Urban Syst 2016;59:25–37. https://doi.org/10.1016/j.compenvurbsys.2016.04.005.
[33] Dubey S, Sarvaiya JN, Seshadri B. Temperature dependent photovoltaic (PV) efficiency and its effect on PV production in the world – a review. Energy Procedia 2013;33:311–21. https://doi.org/10.1016/j.egypro.2013.05.072.
[34] Brelsford C, Tennille S, Myers A, Chinthavali S, Tansakul V, Denman M, et al. A dataset of recorded electricity outages by United States county 2014–2022. Sci Data 2024;11:271. https://doi.org/10.1038/s41597-024-03095-5.
[35] Huang Y, Lai D, Liu Y, Xuan H. Impact of climate change on outdoor thermal comfort in cities in United States. E3S Web Conf 2020;158:01002. https://doi.org/10.1051/e3sconf/202015801002.
[36] Jiang A, Zhu Y, Elsafty A, Tumeo M. Effects of global climate change on building energy consumption and its implications in Florida. Int J Constr Educ Res 2018;14(1):22–45. https://doi.org/10.1080/15578771.2017.1280104.
[37] Xue CQ, Zhai H, Roberts J. An urban island floating on the MTR station: A case study of the West Kowloon development in Hong Kong. Urban Design International 2010;15:191–207. https://doi.org/10.1057/udi.2010.21.
[38] A Hong Kong Developer's vision for Miami. Urban Land 2014. https://urbanland.uli.org/development-business/hong-kong-developers-vision-miami (accessed July 14, 2024).
[39] Liu H, Davidson RA, Apanasovich TV. Statistical forecasting of electric power restoration times in hurricanes and ice storms. IEEE Trans Power Syst 2007;22:2270–9. https://doi.org/10.1109/TPWRS.2007.907587.
[40] Do V, McBrien H, Flores NM, Northrop AJ, Schlegelmilch J, Kiang MV, Casey JA. Spatiotemporal distribution of power outages with climate events and social vulnerability in the USA. Nature Communications 2023;14(1):2470. https://doi.org/10.1038/s41467-023-38084-6.
[41] A Wake up Call from Mangkhut https://www.hko.gov.hk/en/Observatorys-Blog/101819/A-Wake-up-Call-from-Mangkhut; 2018. [Accessed 26 June 2024].
[42] Population Profile of Yau Tsim Mong District | District Profile | Kowloon City and Yau Tsim Mong | Districts Services and Information | Public Services | Social Welfare Department. https://www.swd.gov.hk/en/pubsvc/district/kcytm/districtpr/ytmpp/. [Accessed 26 June 2024].
[43] Miami Dade County | Christian Cevallos. https://miami-dade.us/miami-dade-county/. [Accessed 26 June 2024].
[44] Announcement of the ministry of housing and urban-rural development on the publication of the national standard design code for electrochemical energy storage power stations. https://www.mohurd.gov.cn/gongkai/zhengce/zhengcefilelib/201412/20141205_224298.html; 2024. accessed June 26, 2024.
[45] T/CEC 373—2020 fire service technical specification for prefabricated cabin type lithium iron phosphate Battery energy storage stations http://www.cepp.com.cn/ERP_BOOK/xsyg_610/gcgf/202010/t20201029_327905.html; 2024. [Accessed June 26, 2024].
[46] Earth resources observation and science (EROS) center. Collection-2 Landsat 8–9 OLI (Operational Land Imager) and TIRS (Thermal Infrared Sensor) Level-2 Science Products. 2013. https://doi.org/10.5066/P9OGBGM6.

[47] Nichol JE, To PH. Temporal characteristics of thermal satellite images for urban heat stress and heat island mapping. ISPRS J Photogramm Remote Sens 2012;74:153–62. https://doi.org/10.1016/j.isprsjprs.2012.09.007.
[48] Nik VM, Perera ATD, Chen D. Towards climate resilient urban energy systems: a review. Natl Sci Rev 2021;8:nwaa134. https://doi.org/10.1093/nsr/nwaa134.
[49] Zhou Y, Liu XC, Wei R, Golub A. Bi-objective optimization for battery electric bus deployment considering cost and environmental equity. IEEE Transactions on Intelligent Transportation Systems 2020;22(4):2487–97. https://doi.org/10.1109/TITS.2020.3043687.
[50] Rahmani S, Scorzelli R, Ragone F, Fattoruso G, Murgante B. Utilizing spatial multi-criteria analysis to determine optimal sites for green hydrogen infrastructure deployment. In: Marucci A, Zullo F, Fiorini L, Saganeiti L, editors. Innov. Urban Reg. Plan, Cham: Springer Nature Switzerland; 2024. p. 385–96. https://doi.org/10.1007/978-3-031-54096-7_34.
[51] Correa ES, Steiner MT, Freitas AA, Carnieri C. A genetic algorithm for solving a capacitated p-median problem. Numerical Algorithms 2004;35:373–88. https://doi.org/10.1023/B:NUMA.0000021767.42899.31.
[52] Introduction — PyPSA: Python for Power System Analysis. https://pypsa.readthedocs.io/en/latest/getting-started/introduction.html. [Accessed 12 September 2024].
[53] Meng Y, Ma G, Ye Y, Yao Y, Li W, Li T. Design of P2P trading mechanism for multi-energy prosumers based on generalized nash bargaining in GCT-CET market. Appl Energy 2024;371:123640. https://doi.org/10.1016/j.apenergy.2024.123640.
[54] Data | Electricity | 2021 | ATB | NREL https://atb.nrel.gov/electricity/2021/data; 2021. [Accessed 29 April 2024].
[55] Song A, Dan Z, Zheng S, Zhou Y. An electricity-driven mobility circular economy with lifecycle carbon footprints for climate-adaptive carbon neutrality transformation. Nat Commun 2024;15:5905. https://doi.org/10.1038/s41467-024-49868-9.
[56] Woo CK, Ho T, Shiu A, Cheng YS, Horowitz I, Wang J. Residential outage cost estimation: Hong Kong. Energy Policy 2014;72:204–10. https://doi.org/10.1016/j.enpol.2014.05.002.
[57] China light & power company syndicate sustainability report. https://sustainability.clpgroup.com/zh-hk/2023; 2023.
[58] C&SD : Table 915–91201 : Monthly statistics on consumption of electricity and gas by type of users. https://www.censtatd.gov.hk/en/web_table.html?id=127; 2024. accessed July 2, 2024.
[59] Chapter 11: weather and climate extreme events in a changing climate | climate change 2021: the physical science basis https://www.ipcc.ch/report/ar6/wg1/chapter/chapter-11/; 2021. [Accessed 16 June 2024].
[60] Bowen T, Chernyakhovskiy I, Denholm P. Grid-scale battery storage: Frequently asked questions; 2019.
[61] Zhang X, Zhou Y. Life-cycle carbon-intensity mapping for hydrogen-driven energy and economy. Cell Reports Physical Science 2024;5(9):102146.
[62] Zhou Y. Climate change adaptation with energy resilience in energy districts—A state-of-the-art review. Energy and Buildings 2023;279:112649.